Front. Phys., 2014, 9(3): 351–369
DOI 10.1007/s11467-013-0308-x

REVIEW ARTICLE

Applications of carbon nanotubes in high performance lithium ion batteries

Yang Wu, Jiaping Wang*, Kaili Jiang, Shoushan Fan†

Department of Physics and Tsinghua-Foxconn Nanotechnology Research Center, Tsinghua University, Beijing 100084, China

*Corresponding authors. E-mail: *jpwang@tsinghua.edu.cn, †fss-dmp@tsinghua.edu.cn*

Received January 7, 2013; accepted February 20, 2013

The development of lithium ion batteries (LIBs) relies on the improvement in the performance of electrode materials with higher capacity, higher rate capability, and longer cycle life. In this review article, the recent advances in carbon nanotube (CNT) anodes, CNT-based composite electrodes, and CNT current collectors for high performance LIBs are concerned. CNT has received considerable attentions as a candidate material for the LIB applications. In addition to a possible choice for anode, CNT has been recognized as a solution in improving the performance of the state-of-the-art electrode materials. The CNT-based composite electrodes can be fabricated by mechanical or chemical approaches. Owing to the large aspect ratio and the high electrical conductivity, CNTs at very low loading can lead to an efficient conductive network. The excellent mechanical strength suggests the great potential in forming a structure scaffold to accommodate nano-sized electrode materials. Accordingly, the incorporation of CNTs will enhance the conductivity of the composite electrodes, mitigate the agglomeration problem, decrease the dependence on inactive binders, and improve the electrochemical properties of both anode and cathode materials remarkably. Freestanding CNT network can be used as lightweight current collectors to increase the overall energy density of LIBs. Finally, research perspectives for exploiting CNTs in high-performance LIBs are discussed.

Keywords lithium ion battery, carbon nanotube, composite, conductive additive, structural scaffold

PACS numbers 82.47.Aa, 81.05.U-, 81.07.De

Contents

1 Introduction

One of the greatest challenges that the human society faces lies in the discrepancy between the increasing population and limited supply of global energy. Even though the current requirement of the total energy consumption is basically met by burning fossil fuels, the unpredictable effects on the climate cannot be ignored. The development of clean and renewable energy sources has since been seriously considered. Accompanying innovative concepts and advanced understandings in both material physics and chemistry, tremendous progress has been made towards the-state-of-the-art renewable energy technologies, including solar cells, hydrogen storage, bio fuels, thermoelectrics, and batteries. It is universally believed that any breakthrough in the research of renewable energy will reduce the dependence on conventional energy sources.

Amongst all the above mentioned renewable energy technologies, lithium ion battery (LIB) is unique owing to its great portability. At this age, LIBs occupy the largest portion of the commercial battery market to power portable electronics. Next-generation LIBs are expected to have high reversible capacity, superior cycling stability, and excellent rate performance to match the requirements in hybrid/plug-in electric vehicles (HEV/PEV) and grid storage devices in order to decrease the emission from burning gasoline [1–3]. LIB is an electrochemical energy storage device that involves charge transfer across the interface between the electrolyte and the electrode. Applying lithium to develop high performance batteries is motivated by its low standard reduction potential at -3.04 V vs. H^+/H_2, as well as the low density ($0.53\ g\cdot cm^{-3}$). With the same weight, the batteries based on lithium can store more energy than any other types of batteries. The earliest lithium battery was developed based on TiS_2 cathode and Li metal anode by Exxon in 1970s [4]. The commercialization of this lithium battery finally failed for many reasons, such as the high reactivity of lithium to the organic electrolytes, formation of dendrites, and the high flammability of metal lithium [3]. Attempts to solve these safety concerns led to the utilization of carbonaceous materials as anodes. By combining carbonaceous anodes and $LiCoO_2$ cathodes with layered structures that can host lithium, LIBs available in the present market were first commercialized by Sony in 1991 [3, 5, 6].

The working principle of LIBs is illustrated in Fig. 1. Using “lithium ion battery” instead of “lithium battery” is associated with the shuttling of lithium ions between cathodes and anodes [3, 5, 7]. The prevalent cathode material could be lithium containing metal oxides and the anode material is dominated by carbonaceous materials, for instance, $LiCoO_2$ and graphite as shown in Fig. 1. In the charging process, lithium ions are forced to leave those gaps between oxide layers in the $LiCoO_2$ structure under an external electric field and intercalate into the graphite lattice. Note that the term “intercalate” is used more popularly than “insert” in the literature concerning LIBs. The discharging process can be considered as the reverse of charging, in which lithium ions deintercalate from the graphite lattice and are accommodated by the $LiCoO_2$ lattice again. A porous polymer separator electrically insulates the cathode and the anode, and provides channels for lithium ion transfer during the charging/discharging processes. In practice, cathode and anode materials are attached to Al and Cu current collectors, respectively, to improve the electrical conductivity and support the electrodes (not shown in Fig. 1).

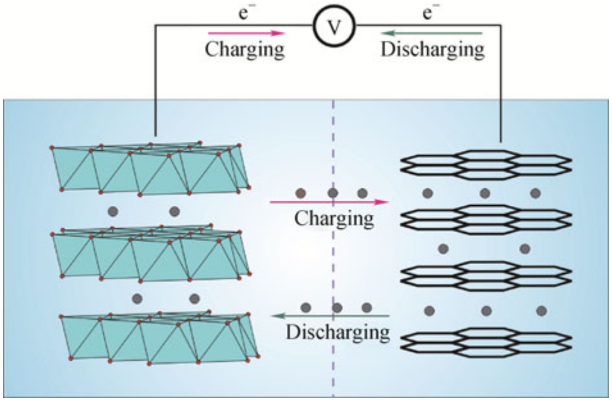

Fig. 1 Illustration of lithium ion batteries. Grey dots represent Li^+.

The performance of LIBs is mainly determined by the intrinsic properties of electrode materials. Carbonaceous materials as anodes for LIBs exhibit significant advantages [9]. As a new member in the carbonaceous material family, carbon nanotube (CNT) is distinguishing in improving the performance of current electrode materials. CNT possesses a one dimensional structure with saturated carbon bonds on the surface [8]. This unique structural feature raises extra potentials beyond a mere lithium storage material. For instance, the large aspect ratio and high electrical conductivity suggest the superiority in forming conductive networks at a rather low loading of CNTs, which will benefit those popular electrode materials based on oxides with low electrical conductivity [9]. CNTs are made of strong sp^2 carbon bonding. Their excellent mechanical properties will be utilized to buffer the volumetric change in the electrodes during charging/discharging processes [10, 11]. CNT networks are excellent scaffold structures to host a wide variety of nano-sized electrode materials. With a similarity in size, the conducting CNT network is very efficient in electron transfer with the active materials. The bind-free composite electrode concept can be embodied in the CNT composite electrodes achieved by either mechanical or chemical attempts, with the CNT network as structural scaffold. Lastly, interlaced CNT films hold promises as lightweight and flexible current collectors.

In this review, we aim to provide a concise but rather comprehensive survey on the applications of CNTs in high-performance lithium ion batteries to the best of our knowledge. This article is arranged as follows: brief discussion on the lithium storage mechanism in carbonaceous materials, the potential of CNTs as conductive additives and structural scaffolds for composite electrodes, the functions of CNTs to template the in-situ growth of electrode materials, and the applications of CNT films as current collectors.

2 Carbonaceous materials as anodes in LIBs

2.1 Lithium storage in carbon

From the view of material scientists, carbon is one of the most abundant elements on the earth with attractive applications in many fields. The reaction of carbon and lithium has been investigated for a long time. Besides the formation of carbides, Li can also insert into the graphite lattice, only resulting in a slight expansion between graphene layers but retaining the integrity of the structure. The very low redox potential of such an insertion process suggests a similar reactivity to that of metallic lithium [12, 13]. Accordingly, this “intercalation” reaction, as termed in many articles, was extensively investigated from 1950s to exploit carbonaceous materials as a safer anode than Li metal in LIBs [14–16]. The intercalation mechanism of lithium storage in the graphite can be understood in terms of the crystal structure. The graphite lattice is constructed via stacking graphene layers in either ABAB $\cdots$ or ABCABC $\cdots$ sequences, corresponding to the dominant hexagonal graphite and the less common rhombohedral graphite [17]. Unlike in-plane carbon atoms, the graphene sheets are held together by the van der Waals forces from delocalized π-p bonds. Such weak interactions between graphene sheets allow for the intercalation of a wide variety of atoms [14]. The intercalation of lithium takes place in different stages because lithium atoms try to occupy distant graphene layers to avoid the static repulsion [Fig. 2(a), (b) and (c)]. As a result, the intercalation process is accompanied with an expansion of the graphite lattice along the c-direction [18–21]. At the fully lithiated stage, lithium atoms will fill in all gaps between graphene layers and associate with only one hexagonal carbon ring. The neighbored graphene layer slides slightly to AA stacking to have each Li atom being sandwiched between hexagonal carbon rings directly facing each other, forming a Li-C_6-Li-C_6 sequence along the c-axis [Fig. 2(d) and (e)]. This structural model corresponding to the fully intercalated graphite has been verified by theoretical studies [22]. According to this model, the chemical composition of graphite at the fully lithiated stage is LiC_6 with a theoretical capacity of 372 mAh·g^{-1}. The access to all nearest neighbor sites is only achieved under extreme synthetic conditions ($\sim$60 kbar, 573 K) [23, 24]. The resulted LiC_2 phase possesses very short Li-Li distances at ca. 2.5 Å and is metastable with respect to the decomposition to intermediate Li-C phases, Li, and LiC_6 at ambient conditions [23].

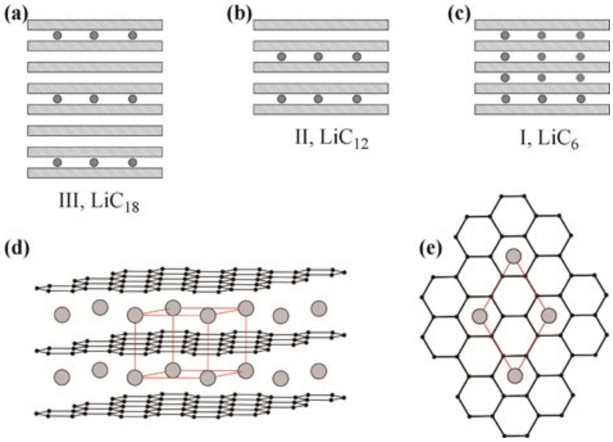

Fig. 2 **(a)**–**(c)** Formation of Li_xC_6 intercalation compounds at different stages with compositions. Graphene layers are drawn as grey bars. Models are redrawn from Ref. [7]. **(d)** Crystal structure of LiC_6, showing AA-stacking of graphene layers. **(e)** Top view of LiC_6. Carbon atoms are plotted with a much smaller size to emphasize the position of intercalated lithium. The unit cell is highlighted in red for both (d) and (e).

In practice, perfect graphite is hard to make because of the easy generation of crystallographic defects by the relative sliding and rotating of graphene layers. The carbonaceous material can be classified into graphitic carbon with a high crystallization state of graphite, and into non-graphitic carbon with varying degrees of misorientation and misfits of graphene layers. The non-graphitic carbon is composed of many graphite crystallites that crosslink with amorphous regions so that it lacks long-range crystallographic orientation along the c-axis. The planar hexagonal network is still appreciable under structural characterization tools such as TEM [25, 26]. The practical lithium storage capacity of non-graphitic carbon is affected by the degree of deviation to the ideal graphite structure. Non-graphitic carbon can be grouped into “soft” carbon and “hard” carbon. In soft carbon, the crosslinking between those graphitic regions is weak and the graphite structure can be developed upon heating. In contrast, the graphitic regions in hard carbon are immobilized due to the strong crosslinking. No distinguishable development of graphite structures is observed in hard carbon even at very high temperatures ($\sim$3000 °C) [27]. The reversible capacity of soft carbon is always less than 372 mAh·g^{-1}. This is because the stoichiometric factor “x” in the end compound “Li_xC_6” is smaller than “1” [28]. In fact, the lack of long-range order in the stacking of graphene layers and the crosslinking between graphite crystallites are barriers to the shift to the necessary AA-stacking for lithium intercalation. The contribution from the amorphous part of soft carbon is related to the history of heat treatments [29, 30]. For hard carbons, the lithium storage capacity is higher than that of ideal graphite. Mechanisms to explain this higher capacity have been proposed by researchers. For example, micropores and micro cavities can serve as reservoirs to accommodate lithium [31]. Some hard carbons show high capacities at very low potential just a few mVs above $\mathrm{Li}^+/\mathrm{Li}$. Dahn suggested that lithium can be adsorbed on both sides of the graphene layers, which were randomly arranged like "house of cards" [32]. The introduction of heteroatoms, such as B, Si, P, etc., can also lead to changes in both specific capacity and charge potential [33–35]. However, a model that can elucidate the heteroatom effects has not yet been established very well. Even though hard carbons deliver higher capacities, novel ideas and projects that address soft carbons are still attractive. This is due to several drawbacks of the hard carbon material. i) There is always an extremely high irreversible capacity that will consume a large amount of lithium. ii) The hysteresis between charging and discharging indicates energy losses during cycling. iii) Li deposition at shallow potentials will lead to unwanted plating of lithium metals, being a safety concern that has to be taken into account in the LIB manufacturing [36, 37].

2.2 CNTs as a lithium storage material

CNT can be regarded as a roll-up of graphene layers to form a seamless cylinder capped with fullerenes. The number of concentric graphene layers groups it into single-walled carbon nanotube (SWCNT) and multi-walled carbon nanotube (MWCNT). The spacing of graphene layers in MWCNTs is 0.34 nm, close to that of graphite. This characteristic of the structure of CNT was first observed by high resolution transmission electron microscopy (HRTEM) in 1991 [38]. With a unique structure, CNTs display quite distinctive electrochemical properties. In an ideal CNT, the graphene layer is closed and there is no structural opening from the edge direction as in the graphitic crystallites. The diffusion of lithium ions can be assisted only by defects on the CNT structure. To illustrate the mechanism of lithium ion storage of CNTs, many theoretical studies were carried out to address the kinetics and thermodynamics of the lithium insertion [39–42]. Peculiarly important is the existence of morphological defects. In theoretical attempts, carbon atoms on the wall of CNTs were artificially removed to form defected rings with more than 6 carbon atoms. The results showed that the diffusion of lithium was not energetically favored until the ring-member increased to 9. The energy barrier of lithium ion diffusion through an enneagon, the 9-membered ring, was calculated as 9.69 $\mathrm{kcal\cdot mol^{-1}}$ [41]. Any carbon rings that consist of more than 9 carbon atoms will have negligible restrictions to the penetration of lithium ions.

As an important member in the family of carbon, the possibility of CNT in regard to potential anode material has aroused great interests. The lithium storage capacity of a variety of MWCNTs and SWCNTs has been investigated extensively [43–52]. The amount of lithium that CNT can store is related to the concentration of its structural defects. Therefore, CNTs from different sources revealed a wide range of reversible capacities. Pristine aligned CNTs synthesized via a chemical vapor deposition (CVD) method [53, 54] possessed a clean surface with a small concentration of defects, which was evidenced by the low $\mathrm{I}_D/\mathrm{I}_G$ratio in the Raman spectrum (Fig. 3). Such raw CNTs displayed a reversible capacity of 160 $\mathrm{mAh\cdot g^{-1}}$ in the voltage range of 0.01–2 V vs. $\mathrm{Li}^+/\mathrm{Li}$, much lower than that of graphite (Fig. 3). Similarly, CNT arrays exhibited a reversible capacity of 200 $\mathrm{mAh\cdot g^{-1}}$ and good cycle and rate performance [55]. Free-standing CNT paper and CNT-carbon black mat were also explored as anodes, where metal current collectors were not necessary anymore due to the conductive and self-sustained property of the CNT network [56–58]. Such anodes displayed a reversible capacity of less than 300 $\mathrm{mAh\cdot g^{-1}}$. In some publications, the capacity of CNTs exceeded the value in terms of the composition of $\mathrm{LiC_6}$ compound [44, 45, 59–65]. The excess in the capacity can be attributed to the defects introduced to CNTs by mechanical or chemical processes. Upon a ball-milling process, the capacity of SWCNT bundles was increased over 1000 $\mathrm{mAh\cdot g^{-1}}$ [45]. This increase can be interpreted as a result of the effective shortening in the length and the opening of the ends of CNTs, which favored the lithium diffusion into the CNTs. The extra capacity may also result from the lithium storage in spaces within CNT bundles [61, 62, 65]. As other carbonaceous materials, doping B or N atoms may also affect the capacity [40, 66, 67]. Although the specific capacity of CNTs can be increased after certain mechanical or chemical processes, there are still no conclusive results. One drawback for CNT anodes is that it did not display a voltage plateau, which reminds us the potential profile of hard carbon. This similarity, along with the high irreversible capacity in initial cycles, indicates that the lithium storage of CNTs may be determined by the amorphous feature such as structural defects, rather than the intercalation into graphite crystallites. The efficiency of lithium storage in CNTs may still remain low because of the inevitable loss between the input and the output energies upon the hysteresis loop in each of the charging/discharging cycles. To this end, there is still lack of clear conclusions regarding the practical reversible capacity of CNTs. However, the

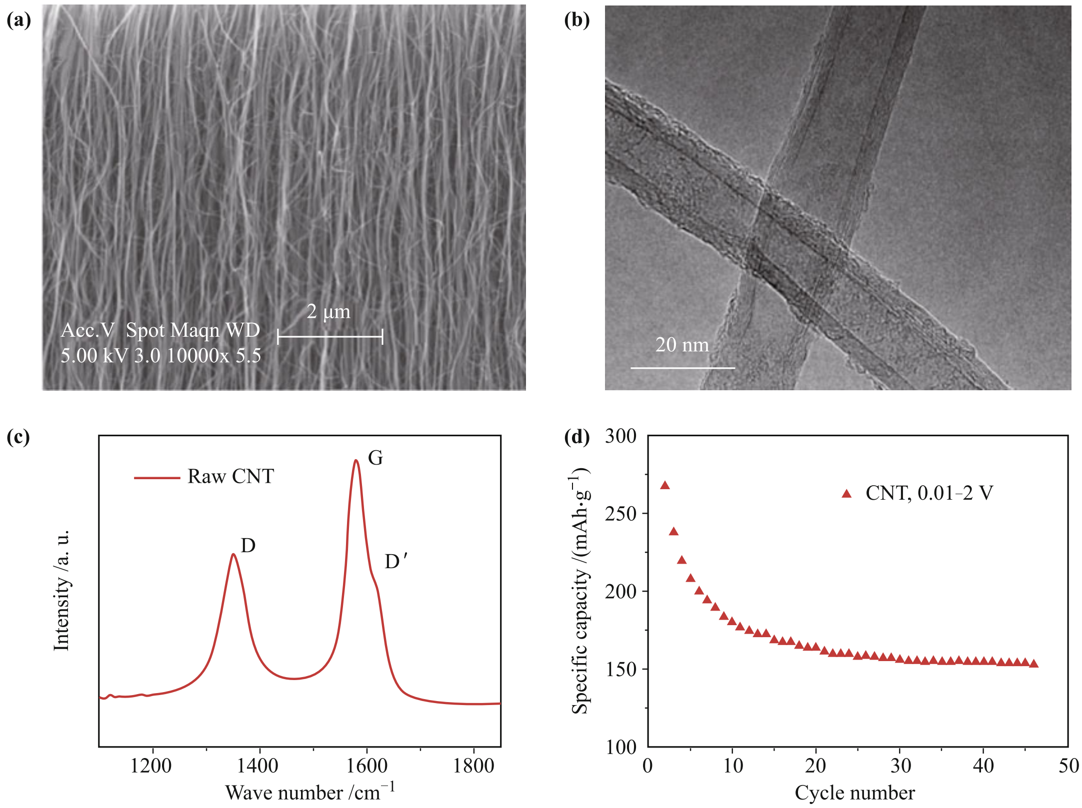

Fig. 3 **(a)** SEM image of aligned CNT array. **(b)** TEM image of individual CNTs (courtesy of Dr. Yuquan Wang). **(c)** Raman spectrum of CNTs. **(d)** Cyclic performance of as-prepared CNTs from 0.01–2 V vs. Li^+/Li.

and electrical properties of CNTs give rises to additional applications beyond an anode material.

3 Beyond anode materials: CNTs as conductive additives and structural scaffolds

Many electrode materials are oxides with poor conductivity. The performance of such electrode materials highly relies on the adequate addition of carbon conductive additives. The high electrical conductivity, large aspect ratio, excellent mechanical properties, and high chemical stability suggest CNTs as a distinctive choice for improving electrochemical properties of both cathodes and anodes [8–11]. Compared with the percolative paths formed by traditional carbon conductive additives such as carbon black and graphite powders, CNTs with large aspect ratios (typically 10^4 or higher) are more effective to form a continuous and conductive network throughout the composite and to gain a much lower percolation threshold. Accordingly, the conductivity and electrochemical properties of the electrodes can be improved at a smaller amount of CNT, leading to a higher gravimetric capacity and power density for the entire electrode. Another significance of CNTs arises from their applications as structural scaffolds in composite electrodes. Because of the excellent mechanical properties of CNTs, the conductive bridges within the composite electrodes can be preserved even when any volumetric change occurs during the lithiation and delithiation processes, resulting in better cycling stability and rate performance.

As to composite electrodes, homogeneous dispersion of CNTs in the active material matrix is very crucial, since non-uniform spatial distribution of the conductive fillers will result in heavy polarization as well as severe capacity fading of the composite electrodes. CNTs can be incorporated with active particles by mechanical approaches such as blending, spraying, and ultrasonication, etc. Alternatively, composite electrodes can also be obtained by in-situ growth of anode or cathode materials on CNTs in either solution or vapor based methods. Synthesis and properties of CNT composite electrodes achieved by these two kinds of approaches will be reviewed respectively.

3.1 CNT composite electrodes by mechanical approaches

Many research efforts involve the incorporation of CNTs with active electrode material particles by mechanical approaches, such as blending and ball milling, resulting in CNT composite electrodes with higher conductivity, higher specific capacity, better cycling stability, and improved rate performance than those with carbon black. For example, in $LiFePO_4$-MWCNT composite cathodes, $LiFePO_4$ particles were connected with a three-dimensional conductive network structure formed by MWCNTs, which can improve electron transport and electrochemical activity effectively [68–72]. The $LiFePO_4$-MWCNTs composite with loading of MWCNTs ranging from 4 wt% to 10 wt% exhibited higher specific capacity, better cycling stability, and improved rate capability than pure $LiFePO_4$ or $LiFePO_4$-carbon black cathodes. MWCNTs have also been widely used as effective conductive additive in $LiCoO_2$, $LiMn_2O_4$, $LiNi_{0.7}Co_{0.3}O_2$, $LiNi_{1/3}Co_{1/3}Mn_{1/3}O_2$, Si, and graphite electrodes, showing improvements in specific capacity, cycling stability, and rate performance [73–80].

Applying CNTs as a sole kind of conductive additives may not be effective to achieve a decent surface coverage on active materials. This problem can be circumvented by a strategy of hybrid conductive agents, which contain both CNTs and carbon blacks powders. CNTs with large aspect ratios favor the electron transfer among multiple particles of the active material along the axial direction of CNTs, but do not provide efficient surface coverage on individual active particles. In comparison, it is easier for round-shaped carbon black powders to provide a conductive layer covering individual active particles. Therefore, with the hybrid conductive agent consisting of fillers with a wide range of aspect ratios, charge transfer pathways can be supplied by both linking multiple active particles in the long range and crossing the surface of individual active particles in the short range. The hybrid CNT-carbon black conductive additives have been integrated into composite $LiCoO_2$ electrodes by mechanical blending and exhibited higher conductivity, better cycling stability, and rate performance than the electrodes containing a single type of conductive agents [75, 81]. Generally speaking, CNTs with large aspect ratios always suffer from agglomeration to a certain extent. We demonstrated that continuous CNT films drawn from super-aligned CNTs (SACNT) arrays with an end-to-end joining mechanism [53, 54, 82, 83] can be cold rolled into the $LiCoO_2$-carbon black composites to avoid agglomeration of CNTs [84]. The composite cathodes containing homogeneous and hybrid SACNTs (less than 0.01 wt%)-carbon black conductive network exhibited reduced percolation threshold, increased conductivity, much better cycling and rate performances compared with the $LiCoO_2$-carbon black cathodes (Fig. 4).

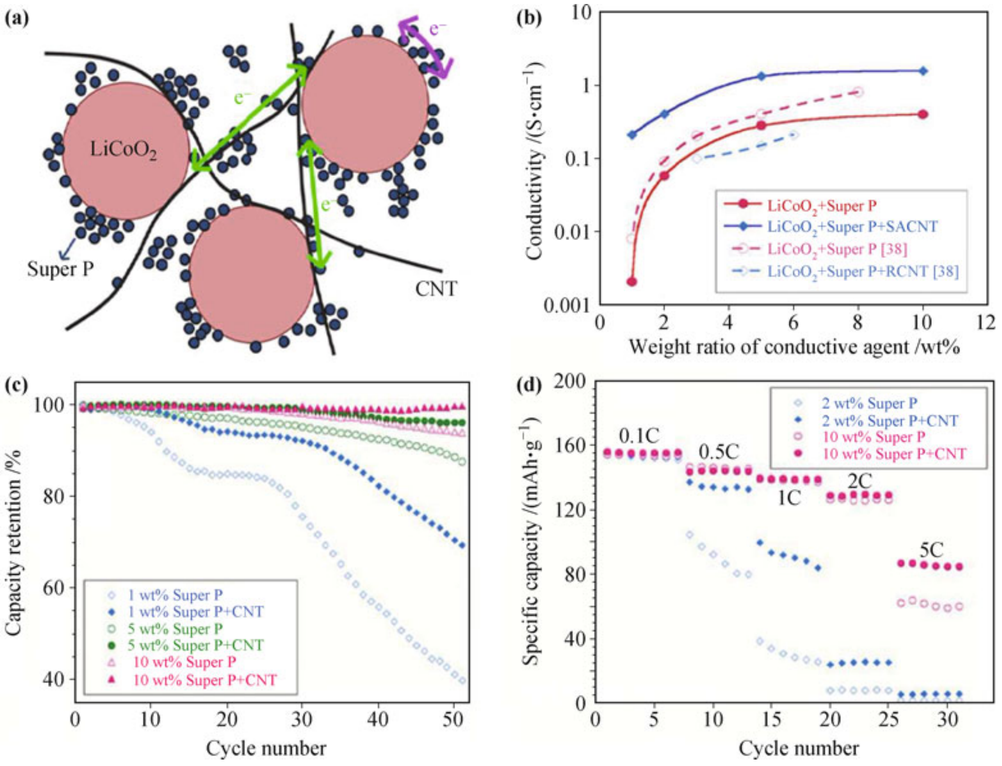

Fig. 4 **(a)** Schematic of long-range and short-range conductive pathways by a hybrid Super P-SACNT network for the $LiCoO_2$ matrix. **(b)** The conductivity of the $LiCoO_2$-Super P and $LiCoO_2$-Super P-SACNT cathodes at different loading of conductive agents. **(c)** Cycling and **(d)** Rate performance of the $LiCoO_2$-Super P and $LiCoO_2$-Super P-SACNT composite cathodes, respectively [84]. Reproduced from Ref. [84], Copyright © 2013 Elsevier.

In the above-mentioned work, CNTs mainly serve as the conductive additive. Binders such as polytetrafluoroethylene (PTFE) or polyvinylidene fluoride (PVDF), which are electrochemically inactive, are commonly required to bind the active materials and conductive additives together. The insulating binders have no benefits in regard to the overall energy density. To eliminate binders, an ultrasonication and co-deposition (USCD) method was developed to fabricate high performance $LiCoO_2$-CNT and $LiMn_2O_4$-CNT electrodes (Fig. 5) [85]. The ideas of using CNTs as both conductive additive and structural scaffold were achieved by constructing a continuous and conductive three-dimensional CNT framework via ultrasonication to embed active material particles. Note that only super-aligned CNTs with very clean surface and strong van der Waals forces among tubes can form the continuous network upon ultrasonication. Binder-free cathodes with excellent flexibility and conductivity displayed much better cycling stability and greater rate performance than classical cathodes with binder. Furthermore, the absence of binder is remarkable for high energy density batteries. The binder-free $LiCoO_2$-3 wt% SACNT composite showed an impressive 20.6% increase in specific mass capacity and 64% increase in specific volume capacity than the optimized classical $LiCoO_2$-10 wt% Super P cathode with binder. The USCD procedure was very fast (10 minutes of ultrasonication) and easy for large-scale production of various kinds of CNT-based composite electrodes.

Binder-free CNT composite electrodes fabricated by other mechanical approaches have also been enriched in the literature [86–88]. For instance, by dropping TiO_2 nano-crystal suspension in toluene on a CNT paper containing ultra-long CNTs with a length of 5 mm, intimate contacts between TiO_2 and CNTs were achieved in combining with vacuum infiltration [87]. Upon solvent evaporation and sintering, the TiO_2 nanoparticles were assembled on CNTs, forming conformal mesoporous TiO_2 coatings on CNTs, which ensured effective electron transport between the CNT scaffold and TiO_2 nanoparticles. The porous channels in the CNT scaffold provided pathways for effective ion transport. Therefore, the flexible TiO_2-CNT composite electrodes demonstrated excellent performance because of the effective pathways for charge and ion transports and the robust scaffold structures. There has also been an attempt to prepare biscrolled $LiFePO_4$/CNT composite yarns for use as binder-free cathodes. $LiFePO_4$ particles were first dispersed in isopropanol by ultrasonication and then deposited onto MWCNT films by vacuum-assisted filtration. Upon twist

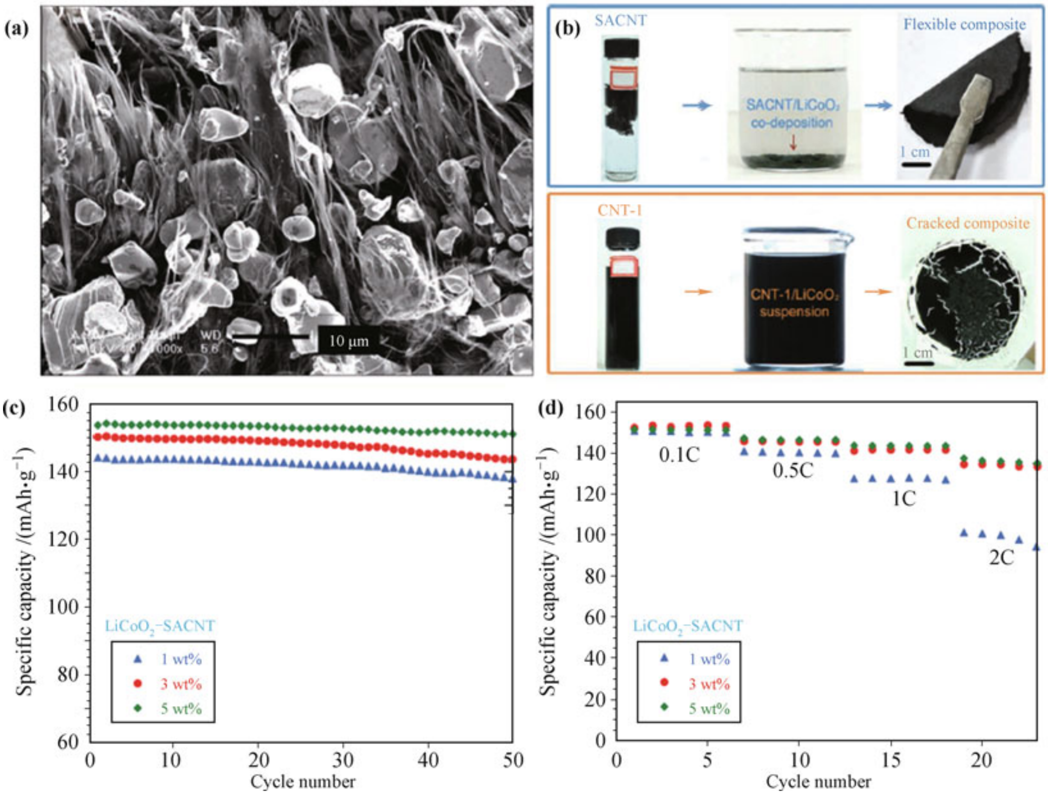

Fig. 5 **(a)** Cross-sectional SEM image of a $LiCoO_2$-1 wt% SACNT composite. **(b)** Features of composite electrodes prepared by the UCSD method with different types of CNTs. **(c)** Cycling (0.1 C) and **(d)** Rate performance of the binder-free $LiCoO_2$ -SACNT composite cathodes. Reproduced from Ref. [85], Copyright © 2012 Wiley-VCH.

insertion in a liquid bath, $LiFePO_4$/MWNTs biscrolled yarns were produced, which displayed reasonable rate performance [86].

3.2 In-situ growth of electrode material on CNTs

The chemical inertness of carbon enables a great viability of CNTs in a wide variety of chemical reactions. Accordingly, the strategy of in-situ growth of anode or cathode materials on CNTs has been extensively explored and results in a vast number of composite electrodes. The growth of electrode materials can be implemented in both solution phases or in gaseous phases. In the previous section, we have discussed recent updates on making CNT composite anodes and cathodes through mechanical approaches. All successful methods towards CNT composite electrodes have to provide intensive energetic inputs to overcome the van der Waals attractions among CNTs. Surfactants or mild surface oxidation becomes sometimes necessary to weaken or alter the interaction among CNTs. Adequate surface modification of CNTs can be achieved by coatings due to the in-situ growth. Thus, the importance for this strategy may not only lie in the effective fabrication of composite electrodes, but also result in rich surface chemistry that benefits the dispersion of CNTs and chemical interactions between CNTs and electrode materials.

The nano-scaled dimension of the material has shown great impacts on the properties. With respect to electrochemistry, nanomaterials show indeed potentials in high-performance LIBs because their reduced dimensions shorten the diffusion length of Li^+ and enable high rate capability [89]. Solution-based chemistry has shown remarkable versatility in synthesizing nano-sized anode materials on CNTs. Owing to the great capability to alloy large amounts of lithium, p-block metals are of great interests as potential replacements to graphite in commercial LIBs. For example, $Li_{4.2}Sn$ and $Li_{4.4}Si$ correspond to a specific capacity of 960 $mAh\cdot g^{-1}$ and 4200 $mAh\cdot g^{-1}$, respectively, far beyond those of commercial graphite (372 $mAh\cdot g^{-1}$ in theory) [89, 90]. By choosing adequate salts such as $SnCl_4$, deposit of tin on CNTs electrochemically is successful to improve the capacity of anodes [91]. High lithium storage capacity can also be fulfilled by a combination of two or more metal species that alloy with lithium. SnSb (<50 nm) and Sn_2Sb nanoparticles (100–200 nm) were coated on CNTs by reductive precipitation of metal chloride salts such as $SnCl_2$ and $SbCl_3$ within a CNT suspension [92, 93]. The reduction of metal ion can be catalyzed by the conductive CNTs. Thus, the continuous precipitation of metal is preferential on the surface of CNTs. The applications of Sn-Sb alloy nanoparticles have since been extended substantially to electrochemical energy storage. Even though the improvement in anode capacity by depositing metals on CNTs has been demonstrated effective, one drawback that we are concerned about is the dramatic volumetric change during the formation of lithium alloy [94, 95]. To circumvent this problem, Kumar *et al.* filled tin into CNTs to reduce the possibility of pulverization as a consequence of lithiation [96]. The capacity can be maintained at 800 $mAh\cdot g^{-1}$ for at least 40 cycles. To enable the tin-fill, vigorous oxidation of CNTs in concentrated nitric acid was a prerequisite to open the ends. Similarly, molten SnSb can be encapsulated inside CNTs, forming SnSb nanorods with CNT shells upon cooling [97]. The CNT shells can improve both the electrical conductivity and mechanical integrity of the SnSb nanorods during cycling. Another way to ease the volumetric expansion is to dilute the active metal, such as Sn, into an inactive matrix composed of another metal that will not alloy with lithium. Examples of Sn-Co and Sn-Cu alloys were reported [98, 99]. Lastly, there are a significantly less number of publications describing in-situ growth of Si and Si-based alloys on CNTs by solution approaches, because Si cations cannot exist in any aqueous solutions. However, by involving a supercritical process in toluene, Chan *et al.* fabricated silicon-coated MWCNTs, which displayed a specific capacity as high as 1500 $mAh\cdot g^{-1}$ [100]. The carbon coating by the pyrolysis of sugar was a critical step for obtaining stable cycling performance. Adopting diazonium chemistry, pre-synthesized Si nanoparticles can also be grafted on the surface of MWCNTs with strong covalent bonding [101].

SnO_2 is a promising type of anode material. The homogeneous nano-coating of SnO_2 on CNTs can be achieved by solution-based methods, such as hydrothermal process, solvothermal process, and sol-gel process, etc. [102–111]. A SnO_2/MWCNT composite was synthesized in combining with carboxymethyl cellulose as a binder hydrothermally and delivered a reversible capacity of 473 $mAh\cdot g^{-1}$ for at least 100 cycles [104]. Wen *et al.* reported in-situ hydrothermal growth of mesoporous SnO_2 on MWCNTs [103]. In this approach, cetyltrimethylammonium bromide was employed as a structure-directing agent. The mesoporous SnO_2-MWCNTs composites exhibited higher reversible capacity and better rate capability than those of pure SnO_2. The improvement of the hybrid mesoporous composite was related to the hollow structure, strength and flexibility, excellent electrical conductivity, and large surface area [Fig. 6(a) and (b)]. Zhang *et al.* used poly(vinyl-pyrrolidone) as a linking agent to anchor SnO_2 nanoparticles on cross-stacked CNT sheets, which were assembled from CNT films dir-

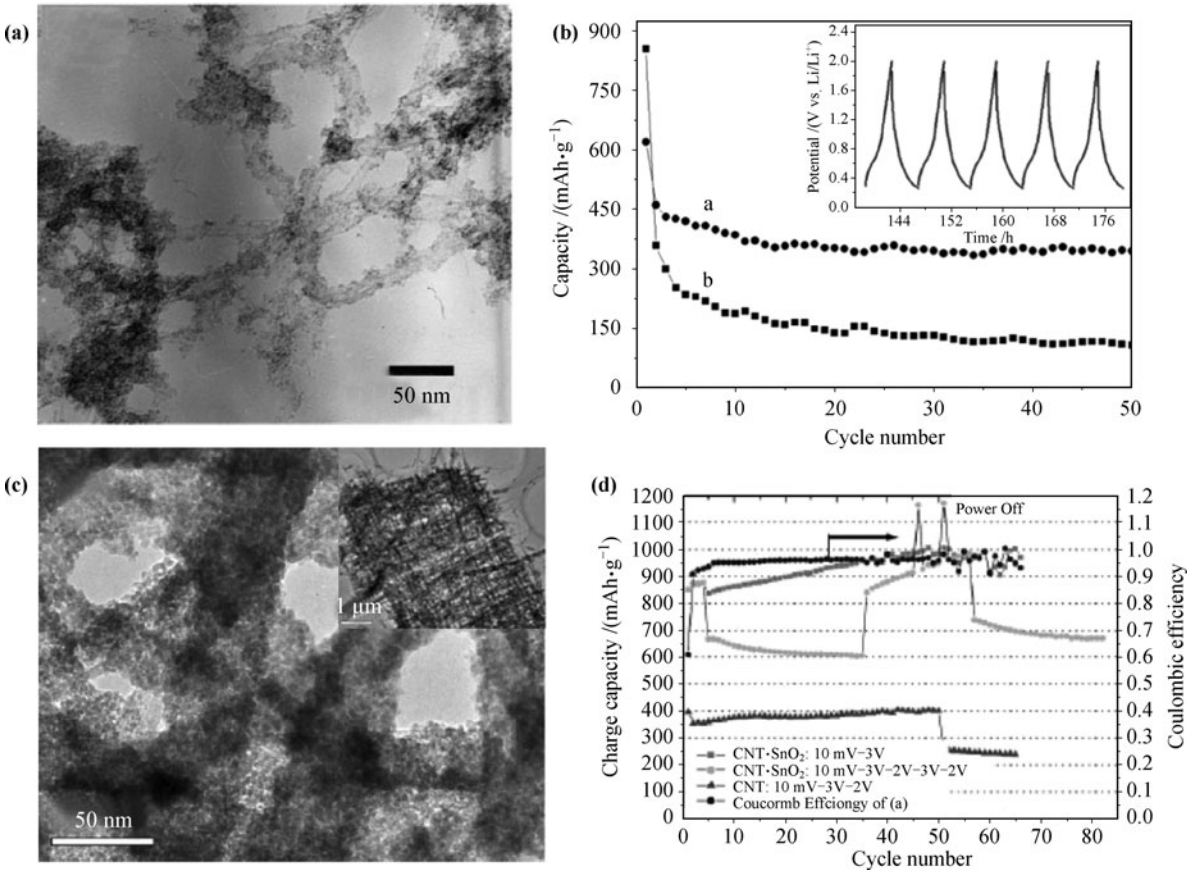

Fig. 6 **(a)** TEM image of MWCNT-mesoporous SnO_2 (m-SnO_2). **(b)** Cycling performance of a, MWCNTs and m-SnO_2, and b, m-SnO_2. Inset: voltage profiles MWCNTs and m-SnO_2. Reproduced from Ref. [103], Copyright © 2007 Wiley-VCH. **(c)** TEM images of cross-stacked CNT sheets loaded with SnO_2 nanoparticles. **(d)** Cycling performance of the composite electrodes at different voltage windows. Reproduced from Ref. [105], Copyright © 2009 Wiley-VCH.

ectly drawn from as-grown super-aligned CNT arrays [105]. The formation of SnO_2 was instead carried out in a solid state reaction. Remarkably, this hybrid composite displayed a much higher capacity at 850 mAh·g^{-1} with 100% retention for 65 cycles [Fig. 6(c) and (d)]. This superior performance can be attributed to the ordered and continuous CNT sheets that serve as a conductive network and structural scaffold. The challenge in using cross-stacked CNT sheets in solution-based methods was how to pertain its structure in turbulent systems such as a hydrothermal bath. Another method with great simplicity was to soak such cross-stacked CNT sheets into the aqueous solution of the metal nitrates, which were directly decomposed into oxides by a following annealing step in Ar or N_2. A large variety of metal oxides can be synthesized onto CNTs by this means.

Transition metal oxides, such as Co_3O_4, Fe_2O_3, Fe_3O_4, MnO_2, Mn_3O_4 etc., are another class of material with high lithium storage capacities [112, 113]. Their CNT-based composites were fabricated to explore their potential as anodes for LIBs [114–116]. As earth abundant materials, Fe_3O_4 and Fe_2O_3 are of great interests [114, 117]. Fe_3O_4 nanoparticles were formed along the sidewalls of MWCNTs by the chemical co-precipitation of Fe^{2+} and Fe^{3+} in an alkaline solution [118]. The Fe_3O_4-CNTs composite electrode displayed stable cyclic retention and delivered a high discharge capacity of 656 mAh·g^{-1} at the 145th cycle. A creative study concerned well dispersed Fe_3O_4 nanorods, as the active material, into the SWCNT conductive network [114]. The synthesis involved a hydrothermal step using $FeCl_3$ as the source, followed by a heat treatment to anchor Fe_3O_4 nanorods into the SWCNT network. The SWCNTs benefited both structural integrity and electrical conductivity. With only 5 wt% SWCNTs, the highest reversible capacity was delivered at 1000 mAh·g^{-1} for 100 cycles, suggesting a competitive anode material. What should be noted is the high rate performance. Stable capacities of 800 mAh·g^{-1} and 600 mAh·g^{-1} were delivered at 5C and 10C, respectively. Possible reasons could be the charge transfer between Fe_3O_4 and CNTs, as preliminarily evidenced by the change in the shape of G-bands as well as the shift and the increase in low frequency lines from 1554 to 1538 cm^{-1} in Raman spectra. Therefore, the chemical process potentially bonded the active material and the CNTs. For other transition metal oxides, the MnO_2 nano-flakes/CNT composite was synthesized hydrothermally with little capacity fade for the first 20 cycles [119]. Reddy *et al.* synthesized MnO_2-CNT nanocables. The MnO_2 nanotube was first synthesized in anodic aluminum oxide (AAO) templates and CNTs were then grown inside MnO_2 tubes with a CVD method to form a core-shell structure [115]. The MnO_2-CNT nanocable displayed ~1000 $mAh\cdot g^{-1}$ for initial cycles, which, however, fast decayed to ~500 $mAh\cdot g^{-1}$ after 15 cycles. The core-shell structure of CNT/Co_3O_4 was also reported by Wang *et al.* [120]. By a hydrothermal process, Co_3O_4 nanoparticles were coated on CNTs and the composite electrode exhibited a stable capacity of 530 $mAh\cdot g^{-1}$ over 100 cycles.

Titanium and vanadium oxides exhibit lower capacities in comparison with late transition metal oxides because the lithium storage in such oxides experiences the insertion/intercalation process, instead of the conversion process [121–124]. Consequently, titanium and vanadium oxides show a small polarization in charge/discharge voltage plateaus. Both TiO_2 and $Li_4Ti_5O_{12}$ can be obtained via hydrothermal reactions or sol-gel processes [125–129]. A $Li_4Ti_5O_{12}$-MWCNT core-sheath anode composite, in which TiO_2 was coated on MWCNTs, followed by a hydrothermal process and a post-annealing process to afford $Li_4Ti_5O_{12}$, was reported [126]. Such a coaxial nanocable was capable to show enhanced lithium storage capacities and kinetics. With a higher oxidation state, vanadium oxides display a higher voltage than titanium oxides and therefore are exploited as cathode materials. A sol-gel method was developed to integrate SWCNTs with the V_2O_5 aerogel synthesis [130]. The V_2O_5-SWCNT composite electrodes exhibited specific capacities above 400 $mAh\cdot g^{-1}$ at 1C rate. Recently, a nanocomposite that consisted of interpenetrating V_2O_5 nanowires and CNTs was synthesized [131]. The composite electrode was freestanding and flexible. Its high performance resulted from the CNT conductive network, the interconnected ionic channel, and the mechanical robustness provided by the ultra-long CNTs. With 25 wt% of CNTs, the composite electrode was able to deliver a stable capacity of 120 $mAh\cdot g^{-1}$ for more than 200 cycles at 5C rate. Prevalent cathode materials, such as $LiFePO_4$, $LiNi_xMn_yCo_{1-x-y}O_2$, $LiMn_2O_4$, and $Li_3V_2(PO_4)_3$ etc., were also synthesized on CNTs via in-situ growth in either liquid phase or solid phase attempts [132–138]. To date, there have been a great number of publications regarding composite electrodes utilizing CNTs via solution-based approaches to improve the performance of LIBs. To initiate innovative research, we may suggest a comprehensive understanding in the chemical interaction at the interface and its influence on charge transfers.

In parallel to applying solution-based approaches, the synthesis of active material on CNTs can also be implemented via vapor-based methods such as atomic-layer deposition (ALD) or chemical/physical vapor deposition (CVD/PVD) [139–142]. Conformal coating of V_2O_5 (~17 nm in thickness) on CNT sponge has been reported via an ALD method, in which $VO(OC_3H_7)_3$ was used as the vanadium precursor and deionized (DI) water was used as the oxidizing agent [140]. In the voltage range of 2.1–4.0 V, the MWCNT/V_2O_5 core-shell sponge showed a high and stable areal capacity of 816 $\mu Ah\cdot cm^{-2}$ at 1C rate and an areal capacity of 155 $\mu Ah\cdot cm^{-2}$ at 50C rate, corresponding to a power density of 21.7 $mW\cdot cm^{-2}$

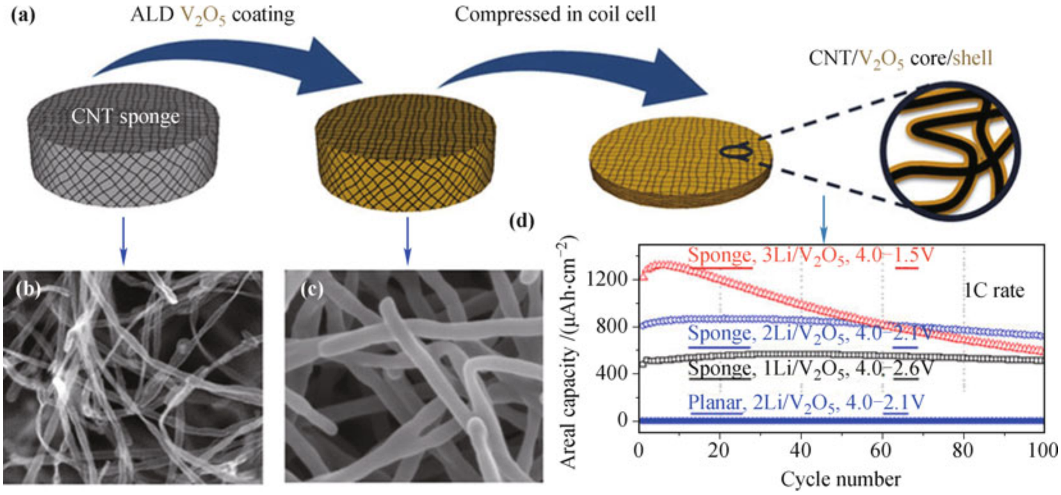

Fig. 7 **(a)** Schematic of the fabrication of V_2O_5-coated MWCNT sponge. **(b)** and **(c)** SEM images of raw-CNTs, CNTs coated with V_2O_5 by ALD, respectively. **(d)** Cycling performance of V_2O_5-MWCNT sponge at different voltage windows. Reproduced from Ref. [140], Copyright © 2012 American Chemical Society.

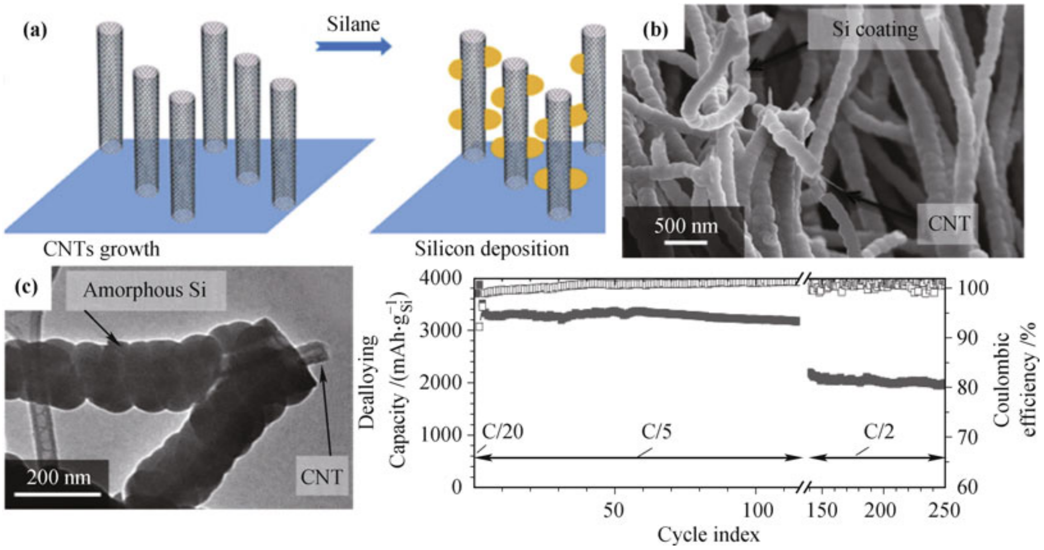

Fig. 8 **(a)** Illustration of the fabrication of Si coating on aligned CNT arrays by CVD. Reproduced from Ref [143], Copyright © 2012 American Chemical Society. **(b)** and **(c)** SEM and TEM images of Si coated VACNTs. **(d)** Specific capacity and Coulombic efficiency at different rates. Reproduced from Ref. [139], Copyright © 2012 Wiley-VCH.

(Fig. 7). In comparison to solution-based methods, e.g. sol-gel process, the deposition in vapor phase does not need elevated temperatures to crystallize the target product. However, because carbon is rather active at elevated temperatures, extra cautions are required to maintain a reductive reaction condition. Even so, attentions on the variation of the oxidation states of metals need to be paid. For performing vapor phase synthesis, the CNT network needs to possess a high porosity to avoid tortuous diffusion paths for the gas molecules. One possible choice is vertically aligned CNT (VACNT) arrays [Fig. 8(a)] [143]. By using such a porous VACNT array substrate, Si nanoparticles were deposited by a CVD method with silane as the precursor [139]. The nanostructured Si/VACNT electrode exhibited reversible capacities of 2050 mAh·g^{-1} at C/2 with a very good capacity retention as shown in Fig. 8. A carbon coating was deposited on the outer layer of Si to guarantee the stable performance. This work represented a thick battery electrode with potentials for large-scale production. Free-standing Si/CNT anodes were made by deposition of Si onto CNT networks with similar CVD methods [143, 144].

Another way to produce highly porous CNT networks that are suitable for vapor phase growth is to draw CNT films, directly from super-aligned CNT arrays. The CNT film is ordered and composed of single-layer parallel CNTs along the drawing direction. Therefore, it can be utilized as a scaffold to host deposits generated from the PVD processes, such as e-beam evaporation and magnetron sputtering. Both methods have been used to produce binary or ternary oxides. The large-scale production of iron oxide onto CNTs can be implemented with a magnetron sputtering process. Sputtering plasma can be generated by two opposite guns using Fe as targets and the CNT film was then gradually drawn through the plasma as shown in Fig. 9(a) [145]. This method provided an easy access to control the thickness of the deposit on the CNT film. Deposited Fe can be spontaneously oxidized to Fe_3O_4. The thickness of the Fe_3O_4 sheath on CNTs can be confined to 5–7 nm, as a function of the drawing speed of the CNT film. The corresponding composite displayed a reversible capacity of 800 mAh·g^{-1} based on its total mass (Fig. 9). The excellent reversibility can be accounted for by the structure integrity as revealed by the post-cycle microscopic studies.

The current trend in the electrode materials for the high performance LIBs is to downsize the material scale to nanometers in order to facilitate the ionic transfer. It is also important to come up with nano-sized conductive additives to deliver electrons to each of the electrochemically active point. This concept can be proofed by in-situ growth of active material directly on CNTs. When enclosed by active materials, the notorious agglomeration problem of CNTs would be mitigated. Finally, the CNT composite electrodes obtained via in-situ synthesis are paradigms in line with the bind-free concept since the active materials strongly interact with the surface of CNTs and hence organic binders become unnecessary.

4 CNT current collectors

The current collector, as an important battery component to hold the electrode material and to conduct

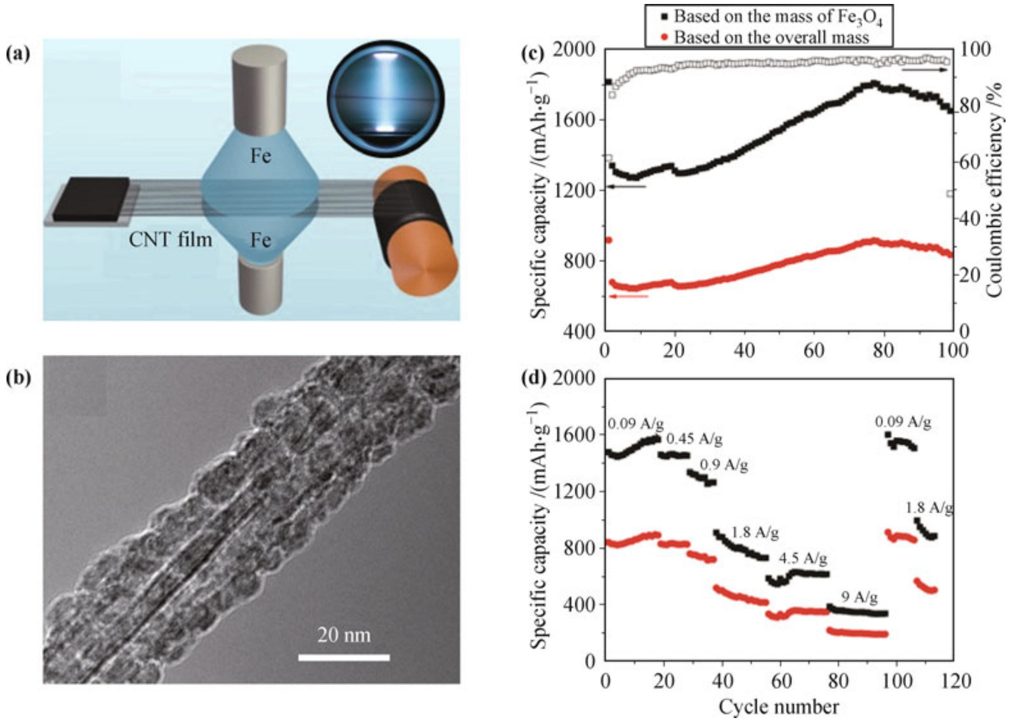

Fig. 9 **(a)** Illustration of the sputtering process to deposit Fe on the CNT film. Inset: A photograph taken in the magnetron sputtering process. **(b)** TEM image of a CNT coated with iron oxides. **(c)** and **(d)** Electrochemical characterizations of cycling and rate performances of Fe_3O_4-CNT electrodes, respectively [145]. Reproduced from Ref. [145], Copyright © 2013 American Chemical Society.

electricity between the electrode material and the electrode lead, would substantially influence the overall performance of LIBs. Current collectors of commercial LIBs are commonly made of metals such as Al and Cu foils. These metal current collectors have no contribution to the overall capacity, but account for 15%–20% of the total mass of the battery [146], which would reduce the energy densities of LIBs severely. In addition, these metal current collectors often exhibit weak adhesion and limited contact area to the electrode material. Detachments of electrode materials from current collectors often result from volumetric change during the charging/discharging processes or bending/folding in flexible LIBs, leading to capacity loss or poor performance at high rates. Moreover, metal current collectors are susceptible to long-term degradations, which may increase the internal impedance and cause capacity losses [147, 148]. Therefore, it is critical to develop a novel type of current collector that is lightweight, thin, mechanically durable, and chemically stable for use in the high-performance flexible LIBs. CNTs with high conductivity, low density, excellent mechanical properties, and high chemical stability are a kind of very promising material for use as current collectors for LIBs.

The interlaced conductive CNT networks are excellent examples for lightweight current collectors for the next-generation LIBs. SWCNT films made from vacuum filtration of SWCNT suspension were originally used as current collectors in Zn-MnO_2 batteries [149]. The high porosity and high surface area of CNTs allow for good integration with the active material particles. The conductivity of such CNT film was as high as 1600–2000 S/cm [149, 150]. Later on, it was demonstrated that aqueous CNT ink with sodium dodecylbenzenesulfonate (SDBS) as a surfactant can be coated onto paper. The highly conductive paper with conformal CNT coating with a low sheet resistance around 10 Ω/sq can serve as lightweight current collectors to replace heavy metal foils in LIBs, leading to higher energy density of the batteries [151].

Afterwards, freestanding CNT films without any supports were developed as current collectors to further increase the energy density of the LIBs [152–154]. CNT films can be made by a spray-painting method for use as current collector [152]. A mixture of 0.5–1 wt% of SWCNTs and 20 wt% of Super P conductive carbon additive were dispersed in 1-methyl-2-pyrrolidone (NMP) by ultrasonication to form viscous and highly conductive inks suitable for spray painting. The spray-painted SWNT-Super P films have a thickness of 30 μm, areal density of 2 mg·cm^{-2}, and sheet resistance of as low as 10 Ω/sq, adequate for the use of current collectors [152]. Alternatively, CNT films can also be fabricated by a doctorblade coating method [153]. Aqueous CNT ink was first coated onto stainless steel substrates, forming CNT thin films with thickness of around 2 μm. After coating electrode slurry onto CNT film and immersing the whole substrate into DI water, the electrode/CNT layer can be peeled off from the stainless steel substrate. The randomly oriented CNT thin film serves as freestanding and lightweight current collector with an areal density of 0.2 mg/cm^2. Electrodes made with such CNT current collectors demonstrated high energy density based on the total mass of the battery.

Highly conductive and freestanding CNT films can also be derived from cross-stacked CNT films drawn from SACNT arrays with smaller thickness and areal density than those of the above-mentioned CNT networks. The SACNT films can be used as lightweight, thin, and flexible current collectors for both graphite anodes and $LiCoO_2$ cathodes to demonstrate remarkable improvements in the battery performance (Fig. 10) [155]. Flexible and freestanding electrodes were fabricated by coating SACNT films with electrode slurry. The thin SACNT films were extremely lightweight with an areal density of as low as 0.04 mg·cm^{-2} and a thickness of less than 1 μm, compared with 16 mg·cm^{-2} and 20 μm for a Cu foil. As a matter of fact, the graphite-CNT electrodes exhibited a more than 180% improvement in gravimetric energy density than the electrodes based on Cu current collectors. The porous structure of the SACNT films enabled easier slurry infiltration, larger contact area, better wetting, stronger adhesion, and lower contact resistance at the electrode/CNT interface. The SACNT films themselves were flexible and strong enough for the structural integrity of the electrodes. Accordingly, any volumetric changes of the electrodes during electrochemical reaction and repeated mechanical deformation in flexible LIBs can be better accommodated, leading to better cycling stability, rate capability, and mechanical durability. Furthermore, fabrication of the SACNT films has been scaled up to meet the industrial requirements, and mass production of lightweight and flexible LIBs with CNT current collectors is potentially feasible.

5 Conclusions and perspectives

It has become a ubiquitous recognition that the future of LIBs should focus on both energy and power density, which is indispensable to the development of electrode materials. The best anode material in LIBs is still dominated by carbonaceous materials. There have been tremendous efforts to explore CNT as a candidate of anode. However, it exhibits quite different behaviors. The lithium storage in CNTs is related to the structural defects and capacitive surface adsorption, rather than the intercalation process that is common in other types of carbonaceous materials. Even though CNT is not one of the best anode materials, it still holds high application potentials due to its superior electrical and mechanical properties.

Accordingly, CNTs will be more likely to play an important supporting role in high-performance LIBs, not involving into the lithium storage directly but providing a conductive network and a structural scaffold for traditional electrode materials. A critical factor in manufacturing battery is the conductivity of the electrode. The addition of a large amount of carbon additive would decrease the energy density of the LIBs. Moreover, the infiltration of liquid electrolytes will be strenuous due to the low porosity and the existence of binders. In contrast, a network formed by CNTs could be both highly porous

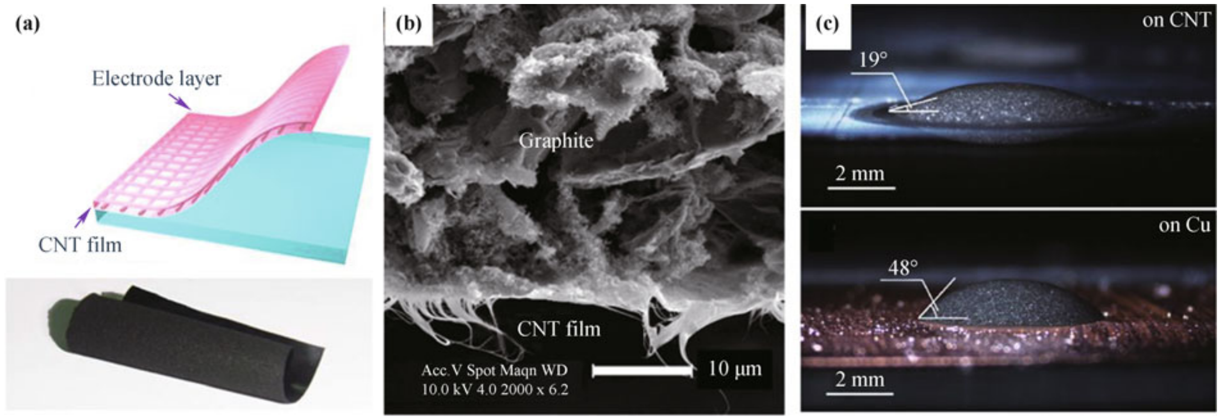

Fig. 10 **(a)** Schematic of the procedure for making flexible electrodes on cross-stacked SACNT films as lightweight and thin current collectors, and a photograph of a freestanding and highly flexible graphite electrode with CNT current collector. **(b)** Cross-sectional SEM image of a graphite electrode with a thin CNT current collector. **(c)** Photographs of graphite slurry droplets (15 μL) on a porous CNT film and a flat Cu foil. Contact angles are highlighted. Reproduced from Ref. [155], Copyright © 2013 Wiley-VCH.

and highly conductive, which will allow for an easy infiltration of electrolytes and minimize the electrical polarization inside the electrodes, particularly for high rate applications.

Another significance that differentiates CNT from other traditional carbon conductive is its capability to construct a structure scaffold to host electrode materials, as a result of its excellent mechanical properties. With strong interactions, such CNT composite electrodes are self-supported and compatible with the idea of binder-free composite electrodes. In fact, inactive organic binders take up to 10 wt% of the electrode. Any removal of inactive component in the electrode is expected to improve both gravimetric energy and power densities. Another advantage is the mechanical flexibility of the CNT scaffolds. Not only can the CNT scaffold host electrode materials, but also buffer the volumetric change accompanying the lithium intercalation/deintercalation processes for electrode materials. The entire morphology of the composite can therefore be maintained even after many cycles, suggesting an excellent long-term stability. The mechanical property of CNTs can also be utilized to make metal-free current collectors with a much lighter weight, higher stability, and better wettability with the slurry of electrodes.

Nanosized material has been the most attractive material system for the current trend in LIBs. The ionic transfer is greatly facilitated in small dimensions, in which the diffusion length of Li^+ ion is drastically shortened. To express the advantages of nanomaterials, current collectors with similar sizes are usually fabricated with sophisticated chemical process. Shifting this strategy to using CNTs to deliver electrons has been demonstrated successful. Nanomaterials can be loaded on the CNT network with both mechanical and chemical approaches. Indeed, the scaffold function of the CNT network also effectively avoids the formation of agglomerates of active materials. As an alternative conductive additive in comparison with carbon black, CNTs will lead to high-performance electrodes in terms of high electric property, large aspect ratios, and ability to construct conductive scaffolds to sustain long-term cycling and high power applications.

In the future, there are still lots of aspects that need to be addressed regarding the applications of CNTs in the next-generation LIBs. The mechanism that underlies the lithium storage in CNT can still be further studied both experimentally and theoretically. The scientific activities always benefit from technologies. The advanced characterization and computational resources would enable the access to more sophisticated modeling. This holds specific importance to the understanding of lithium storage in CNTs towards a clear and convincing conclusion. Interactions between CNTs and active materials are also of great importance. As the electrochemical process concerns both electron and ion transfers, questions such as to what extent the interaction promotes the surface charge transfer would be of great curiosities. The surface chemistry in the CNT-based composites is the second important aspect. Lastly, how to reduce the cost of high-quality CNTs continuously is still an important task for both scientists and engineers.

Acknowledgements This work was supported by the National Basic Research Program of China (Grant No. 2012CB932301), the National Natural Science Foundation of China (Grant Nos. 51102146 and 50825201), and the Chinese Postdoctoral Science Foundation (2012M520261).

References

1. M. Armand and J. M. Tarascon, Building better batteries, *Nature*, 2008, 451(7179): 652
2. B. Dunn, H. Kamath, and J. M. Tarascon, Electrical energy storage for the grid: A battery of choices, *Science*, 2011, 334(6058): 928
3. J. M. Tarascon and M. Armand, Issues and challenges facing rechargeable lithium batteries, *Nature*, 2001, 414(6861): 359
4. M. S. Whittingham, Electrical energy storage and intercalation chemistry, *Science*, 1976, 192(4244): 1126
5. M. S. Whittingham, Lithium batteries and cathode materials, *Chem. Rev.*, 2004, 104(10): 4271
6. K. Ozawa, Lithium-ion rechargeable batteries with $LiCoO_2$ and carbon electrodes: The $LiCoO_2$/C system, *Solid State Ion.*, 1994, 69(3–4): 212
7. M. Winter, J. O. Besenhard, M. E. Spahr, and P. Novak, Insertion electrode materials for rechargeable lithium batteries, *Adv. Mater.*, 1998, 10(10): 725
8. H. Dai, Carbon nanotubes: opportunities and challenges, *Surf. Sci.*, 2002, 500(1–3): 218
9. T. W. Ebbesen, H. J. Lezec, H. Hiura, J. W. Bennett, H. F. Ghaemi, and T. Thio, Electrical conductivity of individual carbon nanotubes, *Nature*, 1996, 382(6586): 54
10. M. F. Yu, O. Lourie, M. J. Dyer, K. Moloni, T. F. Kelly, and R. S. Ruoff, Strength and breaking mechanism of multiwalled carbon nanotubes under tensile load, *Science*, 2000, 287(5453): 637
11. M. M. J. Treacy, T. W. Ebbesen, and J. M. Gibson, Exceptionally high Young's modulus observed for individual carbon nanotubes, *Nature*, 1996, 381(6584): 678
12. R. Fong, U. Sacken, and J. R. Dahn, Studies of lithium intercalation into carbons using nonaqueous electrochemical cells, *J. Electrochem. Soc.*, 1990, 137(7): 2009
13. Z. X. Shu, R. S. McMillan, and J. J. Murray, Electrochemical intercalation of lithium into graphite, *J. Electrochem. Soc.*, 1993, 140(4): 922

14. M. S. Dresselhaus and G. Dresselhaus, Intercalation compounds of graphite, *Adv. Phys.*, 1981, 30(2): 139

15. N. A. Kaskhedikar and J. Maier, Lithium storage in carbon nanostructures, *Adv. Mater.*, 2009, 21(25–26): 2664

16. M. Armand and P. Touzain, Graphite intercalation compounds as cathode materials, *Mater. Sci. Eng.*, 1977, 31(0): 319

17. L. Pauling, The structure and properties of graphite and boron nitride, *Proc. Natl. Acad. Sci. USA*, 1966, 56(6): 1646

18. J. R. Dahn, Phase diagram of $\mathrm{Li}_x\mathrm{C}_6$, *Phys. Rev. B*, 1991, 44(17): 9170

19. N. Kambe, M. S. Dresselhaus, G. Dresselhaus, S. Basu, A. R. McGhie, and J. E. Fischer, Intercalate ordering in first stage graphite-lithium, *Mater. Sci. Eng.*, 1979, 40(1): 1

20. T. Ohzuku, Y. Iwakoshi, and K. Sawai, Formation of lithium-graphite intercalation compounds in nonaqueous electrolytes and their application as a negative electrode for a lithium ion (shuttlecock) cell, *J. Electrochem. Soc.*, 1993, 140(9): 2490

21. K. Persson, Y. Hinuma, Y. S. Meng, A. Van der Ven, and G. Ceder, Thermodynamic and kinetic properties of the Li-graphite system from first-principles calculations, *Phys. Rev. B*, 2010, 82(12): 125416

22. R. C. Boehm and A. Banerjee, Theoretical study of lithium intercalated graphite, *J. Chem. Phys.*, 1992, 96(2): 1150

23. V. A. Nalimova, D. Guerard, M. Lelaurain, and O. V. Fateev, X-ray investigation of highly saturated Li-graphite intercalation compound, *Carbon*, 1995, 33(2): 177

24. V. V. Avdeev, V. A. Nalimova, and K. N. Semenenko, The alkali metals in graphite matrixes-new aspects of metallic state chemistry, *High Press. Res.*, 1990, 6(1): 11

25. Y. Nagata, Y. Ohnishi, H. Hatori, M. Shiraishi, and T. Kajiyama, Carbonization of crystalline polyimide particles, *Kobunshi Ronbunshu*, 1996, 53(5): 302

26. A. Yasuda, N. Kawase, F. Banhart, W. Mizutani, T. Shimizu, and H. Tokumoto, Graphitization mechanism during the carbon-nanotube formation based on the in-situ HRTEM observation, *J. Phys. Chem. B*, 2002, 106(8): 1849

27. R. E. Franklin, Crystallite growth in graphitizing and non-graphitizing carbons, *Proc. R. Soc. Lond. A: Math. Phys. Sci.*, 1951, 209(1097): 196

28. K. Tatsumi, N. Iwashita, H. Sakaebe, H. Shioyama, S. Higuchi, A. Mabuchi, and H. Fujimoto, The influence of the graphitic structure on the electrochemical characteristics for the anode of secondary lithium batteries, *J. Electrochem. Soc.*, 1995, 142(3): 716

29. N. Takami, A. Satoh, M. Hara, and T. Ohsaki, Structural and kinetic characterization of lithium intercalation into carbon anodes for secondary lithium batteries, *J. Electrochem. Soc.*, 1995, 142(2): 371

30. A. Satoh, N. Takami, and T. Ohsaki, Electrochemical intercalation of lithium into graphitized carbons, *Solid State Ion.*, 1995, 80(3–4): 291

31. A. Mabuchi, K. Tokumitsu, H. Fujimoto, and T. Kasuh, Charge-discharge characteristics of the mesocarbon miocrobeads heat-treated at different temperatures, *J. Electrochem. Soc.*, 1995, 142(4): 1041

32. J. R. Dahn, T. Zheng, Y. Liu, and J. S. Xue, Mechanisms for lithium insertion in carbonaceous materials, *Science*, 1995, 270(5236): 590

33. T. D. Tran, J. H. Feikert, X. Song, and K. Kinoshita, Commercial carbonaceous materials as lithium intercalation anodes, *J. Electrochem. Soc.*, 1995, 142(10): 3297

34. C. Kim, T. Fujino, K. Miyashita, T. Hayashi, M. Endo, and M. S. Dresselhaus, Microstructure and electrochemical properties of boron-doped mesocarbon microbeads, *J. Electrochem. Soc.*, 2000, 147(4): 1257

35. M. K. Song and K. T. No, Substitution effect of carbon with group 13, 14, and 15 elements on lithium intercalation in graphite, *J. Electrochem. Soc.*, 2004, 151(10): A1696

36. T. Zheng, Y. Liu, E. W. Fuller, S. Tseng, U. Sacken, and J. R. Dahn, Lithium insertion in high capacity carbonaceous materials, *J. Electrochem. Soc.*, 1995, 142(8): 2581

37. N. Takami, A. Satoh, T. Ohsaki, and M. Kanda, Lithium insertion and extraction for high-capacity disordered carbons with large hysteresis, *Electrochim. Acta*, 1997, 42(16): 2537

38. S. Iijima, Helical microtubules of graphitic carbon, *Nature*, 1991, 354(6348): 56

39. V. Meunier, J. Kephart, C. Roland, and J. Bernholc, Ab initio investigations of lithium diffusion in carbon nanotube systems, *Phys. Rev. Lett.*, 2002, 88(7): 075506

40. Z. Zhou, X. P. Gao, J. Yan, D. Y. Song, and M. Morinaga, A first-principles study of lithium absorption in boron- or nitrogen-doped single-walled carbon nanotubes, *Carbon*, 2004, 42(12–13): 2677

41. C. Garau, A. Frontera, D. Quinonero, A. Costa, P. Ballester, and P. M. Deya, Lithium diffusion in single-walled carbon nanotubes: A theoretical study, *Chem. Phys. Lett.*, 2003, 374(5–6): 548

42. T. Kar, J. Pattanayak, and S. Scheiner, Insertion of lithium ions into carbon nanotubes: An ab initio study, *J. Phys. Chem. A*, 2001, 105(45): 10397

43. G. Maurin, C. Bousquet, F. Henn, P. Bernier, R. Almairac, and B. Simon, Electrochemical intercalation of lithium into multiwall carbon nanotubes, *Chem. Phys. Lett.*, 1999, 312(1): 14

44. A. S. Claye, J. E. Fischer, C. B. Huffman, A. G. Rinzler, and R. E. Smalley, Solid-state electrochemistry of the Li single wall carbon nanotube system, *J. Electrochem. Soc.*, 2000, 147(8): 2845

45. B. Gao, C. Bower, J. D. Lorentzen, L. Fleming, A. Kleinhammes, X. P. Tang, L. E. McNeil, Y. Wu, and O. Zhou, Enhanced saturation lithium composition in ball-milled single-walled carbon nanotubes, *Chem. Phys. Lett.*, 2000, 327(1–2): 69

46. G. L. Che, B. B. Lakshmi, E. R. Fisher, and C. R. Martin, Carbon nanotubule membranes for electrochemical energy storage and production, *Nature*, 1998, 393(6683): 346

47. E. Frackowiak, S. Gautier, H. Gaucher, S. Bonnamy, and F. Beguin, Electrochemical storage of lithium in multiwalled carbon nanotubes, *Carbon*, 1999, 37(1): 61

48. E. Frackowiak and F. Beguin, Electrochemical storage of energy in carbon nanotubes and nanostructured carbons, *Carbon*, 2002, 40(10): 1775

49. B. Gao, A. Kleinhammes, X. P. Tang, C. Bower, L. Fleming, Y. Wu, and O. Zhou, Electrochemical intercalation of single-walled carbon nanotubes with lithium, *Chem. Phys. Lett.*, 1999, 307(3–4): 153

50. G. X. Wang, J. H. Ahn, J. Yao, M. Lindsay, H. K. Liu, and S. X. Dou, Preparation and characterization of carbon nanotubes for energy storage, *J. Power Sources*, 2003, 119-121: 16

51. C. Masarapu, V. Subramanian, H. W. Zhu, and B. Q. Wei, Long-cycle electrochemical behavior of multiwall carbon nanotubes synthesized on stainless steel in Li ion batteries, *Adv. Funct. Mater.*, 2009, 19(7): 1008

52. S. B. Yang, H. H. Song, X. H. Chen, A. V. Okotrub, and L. G. Bulusheva, Electrochemical performance of arc-produced carbon nanotubes as anode material for lithium-ion batteries, *Electrochim. Acta*, 2007, 52(16): 5286

53. K. L. Jiang, Q. Q. Li, and S. S. Fan, Nanotechnology: Spinning continuous carbon nanotube yarns, *Nature*, 2002, 419(6909): 801

54. K. L. Jiang, J. P. Wang, Q. Q. Li, L. A. Liu, C. H. Liu, and S. S. Fan, Superaligned carbon nanotube arrays, films, and yarns: A road to applications, *Adv. Mater.*, 2011, 23(9): 1154

55. H. Zhang, G. P. Cao, and Y. S. Yang, Carbon nanotube arrays and their composites for electrochemical capacitors and lithium-ion batteries, Energy Environ. Sci., 2009, 2(9): 932

56. S. H. Ng, J. Wang, Z. P. Guo, G. X. Wang, and H. K. Liu, Single wall carbon nanotube paper as anode for lithium-ion battery, *Electrochim. Acta*, 2005, 51(1): 23

57. S. Y. Chew, S. H. Ng, J. Z. Wang, P. Novak, F. Krumeich, S. L. Chou, J. Chen, and H. K. Liu, Flexible free-standing carbon nanotube films for model lithium-ion batteries, *Carbon*, 2009, 47(13): 2976

58. B. J. Landi, R. A. Dileo, C. M. Schauerman, C. D. Cress, M. J. Ganter, and R. P. Raffaelle, Multi-walled carbon nanotube paper anodes for lithium ion batteries, *J. Nanosci. Nanotechnol.*, 2009, 9(6): 3406

59. J. Chen, A. I. Minett, Y. Liu, C. Lynam, P. Sherrell, C. Wang, and G. G. Wallace, Direct growth of flexible carbon nanotube electrodes, *Adv. Mater.*, 2008, 20(3): 566

60. G. T. Wu, C. S. Wang, X. B. Zhang, H. S. Yang, Z. F. Qi, P. M. He, and W. Z. Li, Structure and lithium insertion properties of carbon nanotubes, *J. Electrochem. Soc.*, 1999, 146(5): 1696

61. J. Zhao, A. Buldum, J. Han, and J. Ping Lu, First-principles study of li-intercalated carbon nanotube ropes, *Phys. Rev. Lett.*, 2000, 85(8): 1706

62. J. Li, C. Wu and L. Guan, Lithium insertion/extraction properties of nanocarbon materials, *J. Phys. Chem. C*, 2009, 113(42): 18431

63. X. X. Wang, J. N. Wang, H. Chang, and Y. F. Zhang, Preparation of short carbon nanotubes and application as an electrode material in Li-ion batteries, *Adv. Funct. Mater.*, 2007, 17(17): 3613

64. D. T. Welna, L. T. Qu, B. E. Taylor, L. M. Dai, and M. F. Durstock, Vertically aligned carbon nanotube electrodes for lithium-ion batteries, *J. Power Sources*, 2011, 196(3): 1455

65. I. Lahiri, S. W. Oh, J. Y. Hwang, S. Cho, Y. K. Sun, R. Banerjee, and W. Choi, High capacity and excellent stability of lithium ion battery anode using interface-controlled binder-free multiwall carbon nanotubes grown on copper, *ACS Nano*, 2010, 4(6): 3440

66. I. Mukhopadhyay, N. Hoshino, S. Kawasaki, F. Okino, W. K. Hsu, and H. Touhara, Electrochemical Li insertion in B-doped multiwall carbon nanotubes, *J. Electrochem. Soc.*, 2002, 149(1): A39

67. L. G. Bulusheva, A. V. Okotrub, A. G. Kurenya, H. K. Zhang, H. J. Zhang, X. H. Chen, and H. H. Song, Electrochemical properties of nitrogen-doped carbon nanotube anode in Li-ion batteries, *Carbon*, 2011, 49(12): 4013

68. X. L. Li, F. Y. Kang, X. D. Bai, and W. Shen, A novel network composite cathode of $LiFePO_4$/multiwalled carbon nanotubes with high rate capability for lithium ion batteries, *Electrochem. Commun.*, 2007, 9(4): 663

69. B. Jin, E. M. Jin, K. H. Park, and H. B. Gu, Electrochemical properties of $LiFePO_4$-multiwalled carbon nanotubes composite cathode materials for lithium polymer battery, *Electrochem. Commun.*, 2008, 10(10): 1537

70. Y. J. Liu, X. H. Li, H. J. Guo, Z. X. Wang, W. J. Peng, Y. Yang, and R. F. Liang, Effect of carbon nanotube on the electrochemical performance of C-$LiFePO_4$/graphite battery, *J. Power Sources*, 2008, 184(2): 522

71. Y. Feng, The preparation and electrochemical performances of $LiFePO_4$-multiwalled nanotubes composite cathode materials for lithium ion batteries, *Mater. Chem. Phys.*, 2010, 121(1–2): 302

72. T. Muraliganth, A. V. Murugan, and A. Manthiram, Nanoscale networking of LiFePO4 nanorods synthesized by a microwave-solvothermal route with carbon nanotubes for lithium ion batteries, *J. Mater. Chem.*, 2008, 18(46): 5661

73. G. P. Wang, Q. T. Zhang, Z. L. Yu, and M. Z. Qu, The effect of different kinds of nano-carbon conductive additives in lithium ion batteries on the resistance and electrochemical behavior of the $LiCoO_2$ composite cathodes, *Solid State Ion.*, 2008, 179(7–8): 263

74. K. Sheem, Y. H. Lee, and H. S. Lim, High-density positive electrodes containing carbon nanotubes for use in Li-ion cells, *J. Power Sources*, 2006, 158(2): 1425

75. J. H. Park, S. Y. Lee, J. H. Kim, S. Ahn, J. S. Park, and Y. U. Jeong, Effect of conducting additives on the properties of composite cathodes for lithium-ion batteries, *J. Solid State Electrochem.*, 2010, 14(4): 593

76. J. H. Lee, G. S. Kim, Y. M. Choi, W. Il Park, J. A. Rogers, and U. Paik, Comparison of multiwalled carbon nanotubes and carbon black as percolative paths in aqueous-based natural graphite negative electrodes with high-rate capability for lithium-ion batteries, *J. Power Sources*, 2008, 184(1): 308

77. X. L. Li, F. Y. Kang, and W. C. Shen, Multi-walled carbon nanotubes as a conducting additive in a $\mathrm{LiNi_{0.7}Co_{0.3}O_2}$cathode for rechargeable lithium batteries, *Carbon*, 2006, 44(7): 1334

78. X. L. Li, F. Y. Kang, and W. C. Shen, A comparative investigation on multiwalled carbon nanotubes and carbon black as conducting additive in $\mathrm{LiNi_{0.7}Co_{0.3}O_2}$, *Electrochem. Solid-State Lett.*, 2006, 9(3): A126

79. A. Varzi, C. Taubert, M. Wohlfahrt-Mehrens, M. Kreis, and W. Schutz, Study of multi-walled carbon nanotubes for lithium-ion battery electrodes, *J. Power Sources*, 2011, 196(6): 3303

80. J. Y. Eom, J. W. Park, H. S. Kwon, and S. Rajendran, Electrochemical insertion of lithium into multiwalled carbon nanotube/silicon composites produced by ballmilling, *J. Electrochem. Soc.*, 2006, 153(9): A1678

81. C. Sotowa, G. Origi, M. Takeuchi, Y. Nishimura, K. Takeuchi, I. Y. Jang, Y. J. Kim, T. Hayashi, Y. A. Kim, M. Endo, and M. S. Dresselhaus, The reinforcing effect of combined carbon nanotubes and acetylene blacks on the positive electrode of lithium-ion batteries, *ChemSusChem*, 2008, 1(11): 911

82. X. B. Zhang, K. L. Jiang, C. Teng, P. Liu, L. Zhang, J. Kong, T. H. Zhang, Q. Q. Li, and S. S. Fan, Spinning and processing continuous yarns from 4-inch wafer scale super-aligned carbon nanotube arrays, *Adv. Mater.*, 2006, 18(12): 1505

83. K. Liu, Y. H. Sun, L. Chen, C. Feng, X. F. Feng, K. L. Jiang, Y. G. Zhao, and S. S. Fan, Controlled growth of super-aligned carbon nanotube arrays for spinning continuous unidirectional sheets with tunable physical properties, *Nano Lett.*, 2008, 8(2): 700

84. K. Wang, Y. Wu, S. Luo, X. F. He, J. P. Wang, K. L. Jiang, and S. S. Fan, *J. Power Sources*, 2012 (submitted)

85. S. Luo, K. Wang, J. Wang, K. Jiang, Q. Li, and S. Fan, Binder-free $\mathrm{LiCoO_2}$ /carbon nanotube cathodes for high-performance lithium ion batteries, *Adv. Mater.*, 2012, 24(17): 2294

86. M. D. Lima, S. Fang, X. Lepro, C. Lewis, R. Ovalle-Robles, J. Carretero-Gonzalez, E. Castillo-Martinez, M. E. Kozlov, J. Oh, N. Rawat, C. S. Haines, M. H. Haque, V. Aare, S. Stoughton, A. A. Zakhidov, and R. H. Baughman, Biscrolling nanotube sheets and functional guests into yarns, *Science*, 2011, 331(6013): 51

87. Z. Chen, D. Q. Zhang, X. L. Wang, X. L. Jia, F. Wei, H. X. Li, and Y. F. Lu, High-performance energy-storage architectures from carbon nanotubes and nanocrystal building blocks, *Adv. Mater.*, 2012, 24(15): 2030

88. O. Toprakci, H. A. K. Toprakci, L. W. Ji, G. J. Xu, Z. Lin, and X. W. Zhang, Carbon nanotube-loaded electrospun $\mathrm{LiFePO_4}$ /carbon composite nanofibers As stable and binder-free cathodes for rechargeable lithium-ion batteries, *ACS Appl. Mater. Interfaces*, 2012, 4(3): 1273

89. P. G. Bruce, B. Scrosati, and J. M. Tarascon, Nanomaterials for rechargeable lithium batteries, *Angew. Chem. Int. Ed.*, 2008, 47(16): 2930

90. C. M. Hayner, X. Zhao, and H. H. Kung, Materials for rechargeable lithium-ion batteries, Annu. Rev. Chem. Biomol. Eng., 2012, 3: 445

91. S. -D. Seo, G. -H. Lee, A. -H. Lim, K. -M. Min, J. -C. Kim, H. -W. Shim, K. -S. Park, and D. -W. Kim, Direct assembly of tin–MWCNT 3D-networked anode for rechargeable lithium ion batteries, *RSC Advances*, 2012, 2(8): 3315

92. W. X. Chen, J. Y. Lee, and Z. Liu, Electrochemical lithiation and de-lithiation of carbon nanotube-$\mathrm{Sn_2Sb}$ nanocomposites, *Electrochem. Commun.*, 2002, 4(3): 260

93. M. S. Park, S. A. Needham, G. X. Wang, Y. M. Kang, J. S. Park, S. X. Dou, and H. K. Liu, Nanostructured SnSb/carbon nanotube composites synthesized by reductive precipitation for lithium-ion batteries, *Chem. Mater.*, 2007, 19(10): 2406

94. O. Crosnier, T. Brousse, X. Devaux, P. Fragnaud, and D. M. Schleich, New anode systems for lithium ion cells, *J. Power Sources*, 2001, 94(2): 169

95. J. O. Besenhard, J. Yang, and M. Winter, Will advanced lithium-alloy anodes have a chance in lithium-ion batteries? *J. Power Sources*, 1997, 68(1): 87

96. T. P. Kumar, R. Ramesh, Y. Y. Lin, and G. T. K. Fey, Tin-filled carbon nanotubes as insertion anode materials for lithium-ion batteries, *Electrochem. Commun.*, 2004, 6(6): 520

97. Y. Wang and J. Y. Lee, One-step, confined growth of bimetallic tin–antimony nanorods in carbon nanotubes grown*in situ* for reversible $\mathrm{Li^+}$ ion storage, *Angew. Chem. Int. Ed.*, 2006, 45(42): 7039

98. L. Huang, J. S. Cai, Y. He, F. S. Ke, and S. G. Sun, Structure and electrochemical performance of nanostructured Sn–Co alloy/carbon nanotube composites as anodes for lithium ion batteries, *Electrochem. Commun.*, 2009, 11(5): 950

99. K. D. Kepler, J. T. Vaughey, and M. M. Thackeray, $\mathrm{Li}_x\mathrm{Cu_6Sn_5}(0< x <13)$: An intermetallic insertion electrode for rechargeable lithium batteries, *Electrochem. Solid-State Lett.*, 1999, 2(7): 307

100. C. K. Chan, R. N. Patel, M. J. O'Connell, B. A. Korgel, and Y. Cui, Solution-grown silicon nanowires for lithium-ion battery anodes, *ACS Nano*, 2010, 4(3): 1443

101. C. Martin, O. Crosnier, R. Retoux, D. Belanger, D. M. Schleich, and T. Brousse, Chemical coupling of carbon nanotubes

and silicon nanoparticles for improved negative electrode performance in lithium-ion batteries, *Adv. Funct. Mater.*, 2011, 21(18): 3524

102. G. Chen, Z. Y. Wang, and D. G. Xia, One-Pot Synthesis of Carbon Nanotube@SnO_2–Au Coaxial Nanocable for Lithium-Ion Batteries with High Rate Capability, *Chem. Mater.*, 2008, 20(22): 6951
103. Z. H. Wen, Q. Wang, Q. Zhang, and J. H. Li, *In Situ* growth of mesoporous SnO_2 on multiwalled carbon nanotubes: A novel composite with porous-tube structure as anode for lithium batteries, *Adv. Funct. Mater.*, 2007, 17(15): 2772
104. L. Noerochim, J. Z. Wang, S. L. Chou, H. J. Li, and H. K. Liu, SnO_2-coated multiwall carbon nanotube composite anode materials for rechargeable lithium-ion batteries, *Electrochim. Acta*, 2010, 56(1): 314
105. H. X. Zhang, C. Feng, Y. C. Zhai, K. L. Jiang, Q. Q. Li, and S. S. Fan, Cross-stacked carbon nanotube sheets uniformly loaded with SnO_2 nanoparticles: A novel binder-free and high-capacity anode material for lithium-ion batteries, *Adv. Mater.*, 2009, 21(22): 2299
106. J. Xie and V. K. Varadan, Synthesis and characterization of high surface area tin oxide/functionalized carbon nanotubes composite as anode materials, *Mater. Chem. Phys.*, 2005, 91(2–3): 274
107. G. M. An, N. Na, X. R. Zhang, Z. J. Miao, S. D. Miao, K. L. Ding, and Z. M. Liu, SnO_2 /carbon nanotube nanocomposites synthesized in supercritical fluids: highly efficient materials for use as a chemical sensor and as the anode of a lithium-ion battery, *Nanotechnology*, 2007, 18(43): 435707
108. Y. B. Fu, R. B. Ma, Y. Shu, Z. Cao, and X. H. Ma, Preparation and characterization of SnO_2/carbon nanotube composite for lithium ion battery applications, *Mater. Lett.*, 2009, 63(22): 1946
109. G. D. Du, C. Zhong, P. Zhang, Z. P. Guo, Z. X. Chen, and H. K. Liu, Tin dioxide/carbon nanotube composites with high uniform SnO_2 loading as anode materials for lithium ion batteries, *Electrochim. Acta*, 2010, 55(7): 2582
110. C. H. Xu, J. Sun, and L. Gao, Synthesis of multiwalled carbon nanotubes that are both filled and coated by SnO_2 nanoparticles and their high performance in lithium-ion batteries, *J. Phys. Chem. C*, 2009, 113(47): 20509
111. Z. Y. Wang, G. Chen, and D. G. Xia, Coating of multi-walled carbon nanotube with SnO_2 films of controlled thickness and its application for Li-ion battery, *J. Power Sources*, 2008, 184(2): 432
112. P. Poizot, S. Laruelle, S. Grugeon, L. Dupont, and J.-M. Tarascon, Nano-sized transition-metal oxides as negative-electrode materials for lithium-ion batteries, *Nature*, 2000, 407(6803): 496
113. J. Cabana, L. Monconduit, D. Larcher, and M. R. Palacin, Beyond intercalation-based Li-ion batteries: The state of the art and challenges of electrode materials reacting through conversion reactions, *Adv. Mater.*, 2010, 22(35): E170
114. C. M. Ban, Z. C. Wu, D. T. Gillaspie, L. Chen, Y. F. Yan, J. L. Blackburn, and A. C. Dillon, Nanostructured Fe_3O_4/SWNT electrode: Binder-free and high-rate Li-ion anode, *Adv. Mater.*, 2010, 22(20): E145
115. A. L. M. Reddy, M. M. Shaijumon, S. R. Gowda, and P. M. Ajayan, Coaxial MnO_2 /carbon nanotube array electrodes for high-performance lithium batteries, *Nano Lett.*, 2009, 9(3): 1002
116. F. Teng, S. Santhanagopalan, and D. D. Meng, Microstructure control of MnO_2/CNT hybrids under in-situ hydrothermal conditions, *Solid State Sci.*, 2010, 12(9): 1677
117. Z. Wang, D. Luan, S. Madhavi, Y. Hu, and X. W. Lou, Assembling carbon-coated α-Fe_2O_3 hollow nanohorns on the CNT backbone for superior lithium storage capability, *Energy Environ. Sci.*, 2012, 5(1): 5252
118. Y. He, L. Huang, J. S. Cai, X. M. Zheng, and S. G. Sun, Structure and electrochemical performance of nanostructured Fe_3O_4/carbon nanotube composites as anodes for lithium ion batteries, *Electrochim. Acta*, 2010, 55(3): 1140
119. H. Xia, M. O. Lai, and L. Lu, Nanoflaky MnO_2/carbon nanotube nanocomposites as anode materials for lithium-ion batteries, *J. Mater. Chem.*, 2010, 20(33): 6896
120. G. X. Wang, X. P. Shen, J. N. Yao, D. Wexler, and J. Ahn, Hydrothermal synthesis of carbon nanotube/cobalt oxide core-shell one-dimensional nanocomposite and application as an anode material for lithium-ion batteries, *Electrochem. Commun.*, 2009, 11(3): 546
121. A. R. Armstrong, G. Armstrong, J. Canales, R. Garcia, and P. G. Bruce, Lithium-ion intercalation into TiO_2-B nanowires, *Adv. Mater.*, 2005, 17(7): 862
122. P. Liu, S. H. Lee, C. e. Tracy, Y. Yan, and J. Turner, Preparation and lithium insertion properties of mesoporous vanadium oxide, *Adv. Mater.*, 2002, 14(1): 27
123. C. M. Julien, Lithium intercalated compounds, *Mater. Sci. Eng. Rep.*, 2003, 40(2): 47
124. Y. S. Hu, L. Kienle, Y. G. Guo, and J. Maier, High lithium electroactivity of nanometer-sized rutile TiO_2, *Adv. Mater.*, 2006, 18(11): 1421
125. Z. X. Yang, G. D. Du, Z. P. Guo, X. B. Yu, Z. X. Chen, T. L. Guo, and H. K. Liu, TiO_2(B)@carbon composite nanowires as anode for lithium ion batteries with enhanced reversible capacity and cyclic performance, *J. Mater. Chem.*, 2011, 21(24): 8591
126. L. Shen, C. Yuan, H. Luo, X. Zhang, K. Xu, and F. Zhang, In situ growth of $Li_4Ti_5O_{12}$ on multi-walled carbon nanotubes: novel coaxial nanocables for high rate lithium ion batteries, *J. Mater. Chem.*, 2011, 21(3): 761
127. J. J. Huang, and Z. Y. Jiang, The preparation and characterization of $Li_4Ti_5O_{12}$/carbon nano-tubes for lithium ion battery, *Electrochim. Acta*, 2008, 53(26): 7756
128. F. F. Cao, Y. G. Guo, S. F. Zheng, X. L. Wu, L. Y. Jiang, R. R. Bi, L. J. Wan, and J. Maier, Symbiotic coaxial nanocables: Facile synthesis and an efficient and elegant morpholog-

ical solution to the lithium storage problem, *Chem. Mater.*, 2010, 22(5): 1908

129. D. H. Lee, D. W. Kim, and J. G. Park, Enhanced rate capabilities of nanobrookite with electronically conducting MWCNT networks, *Cryst. Growth Des.*, 2008, 8(12): 4506
130. J. S. Sakamoto and B. Dunn, Vanadium oxide-carbon nanotube composite electrodes for use in secondary lithium batteries, *J. Electrochem. Soc.*, 2002, 149(1): A26
131. X. Jia, Z. Chen, A. Suwarnasarn, L. Rice, X. Wang, H. Sohn, Q. Zhang, B. M. Wu, F. Wei, and Y. Lu, High-performance flexible lithium-ion electrodes based on robust network architecture, *Energy Environ. Sci.*, 2012, 5(5): 6845
132. X. M. Liu, Z. D. Huang, S. Oh, P. C. Ma, P. C. H. Chan, G. K. Vedam, K. Kang, and J. K. Kim, Sol–gel synthesis of multiwalled carbon nanotube-$LiMn_2O_4$ nanocomposites as cathode materials for Li-ion batteries, *J. Power Sources*, 2010, 195(13): 4290
133. J. Xu, G. Chen, and X. Li, Electrochemical performance of $LiFePO_4$ cathode material coated with multi-wall carbon nanotubes, *Mater. Chem. Phys.*, 2009, 118(1): 9
134. Y. Zhou, J. Wang, Y. Hu, R. O'Hayre, and Z. Shao, A porous $LiFePO_4$ and carbon nanotube composite, *Chem. Commun.*, 2010, 46(38): 7151
135. C. Ban, Z. Li, Z. Wu, M. J. Kirkham, L. Chen, Y. S. Jung, E. A. Payzant, Y. Yan, M. S. Whittingham, and A. C. Dillon, Extremely durable high-rate capability of a $LiNi_{0.4}Mn_{0.4}Co_{0.2}O_2$ cathode enabled with single-walled carbon nanotubes, *Adv. Energy Mater.*, 2011, 1(1): 58
136. J. J. Chen and M. S. Whittingham, Hydrothermal synthesis of lithium iron phosphate, *Electrochem. Commun.*, 2006, 8(5): 855
137. L. Wang, Y. D. Huang, R. R. Jiang, and D. Z. Jia, Nano-$LiFePO_4$/MWCNT cathode materials prepared by room-temperature solid-state reaction and microwave heating, *J. Electrochem. Soc.*, 2007, 154(11): A1015
138. Y. Q. Qiao, J. P. Tu, Y. J. Mai, L. J. Cheng, X. L. Wang, and C. D. Gu, Enhanced electrochemical performances of multi-walled carbon nanotubes modified $Li_3V_2(PO_4)_3$/C cathode material for lithium-ion batteries, *J. Alloys Compd.*, 2011, 509(25): 7181
139. K. Evanoff, J. Khan, A. A. Balandin, A. Magasinski, W. J. Ready, T. F. Fuller, and G. Yushin, Towards ultrathick battery electrodes: Aligned carbon nanotube-enabled architecture, *Adv. Mater.*, 2012, 24(4): 533
140. X. Chen, H. Zhu, Y. C. Chen, Y. Shang, A. Cao, L. Hu, and G. W. Rubloff, MWCNT/V_2O_5 core/shell sponge for high areal capacity and power density Li-ion cathodes, *ACS Nano*, 2012, 6(9): 7948
141. D. R. Rolison, J. W. Long, J. C. Lytle, A. E. Fischer, C. P. Rhodes, T. M. McEvoy, M. E. Bourg, and A. M. Lubers, Multifunctional 3D nanoarchitectures for energy storage and conversion, *Chem. Soc. Rev.*, 2008, 38(1): 226
142. I. S. Hwang, J. C. Kim, S. D. Seo, S. Lee, J. H. Lee, and D. W. Kim, A binder-free Ge-nanoparticle anode assembled on multiwalled carbon nanotube networks for Li-ion batteries, *Chem. Commun.*, 2012, 48(56): 7061
143. W. Wang and P. N. Kumta, Nanostructured hybrid silicon/carbon nanotube heterostructures: Reversible high-capacity lithium-ion anodes, *ACS Nano*, 2010, 4(4): 2233
144. L. F. Cui, L. B. Hu, J. W. Choi, and Y. Cui, Light-weight free-standing carbon nanotube-silicon films for anodes of lithium ion batteries, *ACS Nano*, 2010, 4(7): 3671
145. Y. Wu, Y. Wei, J. P. Wang, K. L. Jiang, and S. S. Fan, *Nano Lett.*, 2012 (submitted)
146. B. A. Johnson and R. E. White, Characterization of commercially available lithium-ion batteries, *J. Power Sources*, 1998, 70(1): 48
147. P. Arora, R. E. White, and M. Doyle, Capacity fade mechanisms and side reactions in lithium-ion batteries, *J. Electrochem. Soc.*, 1998, 145(10): 3647
148. J. W. Braithwaite, A. Gonzales, G. Nagasubramanian, S. J. Lucero, D. E. Peebles, J. A. Ohlhausen, and W. R. Cieslak, Corrosion of lithium-ion battery current collectors, *J. Electrochem. Soc.*, 1999, 146(2): 448
149. A. Kiebele and G. Gruner, Carbon nanotube based battery architecture, *Appl. Phys. Lett.*, 2007, 91(14): 144104
150. Y. X. Zhou, L. B. Hu, and G. Gruner, A method of printing carbon nanotube thin films, *Appl. Phys. Lett.*, 2006, 88(12): 123109
151. L. B. Hu, J. W. Choi, Y. Yang, S. Jeong, F. La Mantia, L. F. Cui, and Y. Cui, Highly conductive paper for energy-storage devices, *Proc. Natl. Acad. Sci. USA*, 2009, 106(51): 21490
152. N. Singh, C. Galande, A. Miranda, A. Mathkar, W. Gao, A. L. M. Reddy, A. Vlad, and P. M. Ajayan, Paintable battery, *Sci. Rep.*, 2012, 2: 481
153. L. B. Hu, H. Wu, F. La Mantia, Y. A. Yang, and Y. Cui, Thin, flexible secondary li-ion paper batteries, *ACS Nano*, 2010, 4(10): 5843
154. B. J. Landi, M. J. Ganter, C. D. Cress, R. A. DiLeo, and R. P. Raffaelle, Carbon nanotubes for lithium ion batteries, *Energy Environ. Sci.*, 2009, 2(6): 638
155. K. Wang, S. Luo, Y. Wu, X. F. He, F. Zhao, J. P. Wang, K. L. Jiang, and S. S. Fan, Super-aligned carbon nanotube films as current collectors for lightweight and flexible lithium ion batteries, *Adv. Funct. Mater.*, 2013, 23(7): 846